

# **Towards The Synthesis and Evaluation of Naphthalenediimide-Based Anion Sensors**



**A thesis submitted towards partial fulfillment of  
BS-MS dual degree programme**

**by**

**Ashutosh Priyadarshi**

**Under the guidance of**

**Dr. Pinaki Talukdar**

**Assistant Professor**

**Department of Chemistry**

**IISER Pune.**

**Department of Chemistry**

**Indian Institute of Science Education and Research Pune**

## ACKNOWLEDGEMENTS

Foremost, I would like to express my sincere and deepest gratitude to my advisor Dr. Pinaki Talukdar whose personal guidance, support and encouragement throughout my project enable me to write this thesis.

Beside my advisor, I would like to express my warm and sincere thanks to Dr. Harinath Chakrapani for his insightful comments, encouragement and valuable suggestions.

It is a pleasure to thank my fellow lab mates Dnyaneshwar kand, Sharad deshमुख, A. T. Dharma, Kavita Sharma, Satish Malwal, Dinesh Chauhan and Vinayak Khodade for their valuable suggestions and encouragements.

I also want to acknowledge my classmates Harita, Harpreet, Hemant, Prakhar, Rakesh, Stanzin, Vivek and Vedant for making this period joyful.

Last but not the least; I would like thank my family for their consistent unconditional support and inspiring me to achieve new levels of success.

Ashutosh Priyadarshi

## TABLE OF CONTENTS

	<b>Page Number</b>
LIST OF ABRIVIATIONS	III
LIST OF FIGURES	IV
CHAPTER 1: INTRODUCTION	1
CHAPTER 2: DESIGN	7
CHAPER 3: RESULTS AND DISCUSSIONS	10
3.1 Synthesis	10
3.2 Ultra Violet Spectroscopic Studies	14
3.3 Future Prospects	20
CHAPTER 4: EXPERIMENTAL SECTION	23
4.1 Materials and Methods	23
4.2 .Instrumentations	23
4.3 .Synthesis	24
4.4 Spectral Data	28
CHAPTER 5: REFERENCES	39

## LIST OF ABBREVIATIONS

DCM	Dichloromethane
DFT	Density functional theory
DIPEA	N, N- Diisopropylethylamine
DMF	Dimethylformamide
EA	Ethyl acetate
MALDI	Matrix assisted laser desorption / ionization
MeOH	Methanol
NDI	Naphthalenediimide
NMR	Nuclear magnetic resonance
PE	Petroleum Ether
TBACl	Tetrabutylammoniumchloride
TBAF	Tetrabutylammoniumfluoride
TBAI	Tetrabutylammoniumiodide
TEA	Triethylamine

## LIST OF FIGURES

<b>Sr. No.</b>	<b>Figure Caption</b>	<b>Page No.</b>
1.1	Schematic representation of the $\pi$ -stacking	1
1.2	An example of the $K^+$ selective channel through cation- $\pi$ interactions	2
1.3	Schematic diagram of tetranuclear complex $[Cu_4(L1)Cl_4][Cl]_4(H_2O)_{13}$ entrapping $Cl^-$ via anion- $\pi$ interaction	4
1.4	An example of anion- $\pi$ slide based on anion- $\pi$ interaction	5
2.1	The schematic diagram of the synthesized structure with different units involved	8
2.2	The reported triazene based Calixarene	9
2.3	Proposed concept of the anion- $\pi$ interaction	9
3.1	The Absorbance vs. Wavelength plot of the target compound	10
3.2	Absorbance vs. Concentration plot at $\lambda = 357$ nm	15
3.3	Absorbance vs. Concentration plot at $\lambda = 378$ nm	15
3.4	Absorbance vs. Wavelength plot, at different concentration of the tetrabutylammonium Fluoride (TBAF)	16
3.5	Absorbance vs wavelength graph at different concentrations of TBA salts Bromide (above) Iodide (below)	17
3.6	Absorbance vs. wavelength plot at higher concentration of TBAF	18
3.7	Absorbance vs. wavelength plot at higher concentration of TBABr	19
3.8	Absorbance vs. wavelength plot at higher concentration of TBAI	19

*Dedicated to my parents*

# Chapter 1

## Introduction:

The chemistry of non-covalent interactions (supramolecular chemistry) is a highly dynamic interdisciplinary field with imperative applications in chemistry, biology, physics and engineering.<sup>1-2</sup> The domain of non covalent interaction includes highly exploited Hydrogen bonding, ionic interaction, van der waals interaction, hydrophobic interactions,  $\pi$ -staging, and cation / anion- $\pi$  interactions. Usually these interactions are much weaker than the single covalent bonds and are transient in nature. One of the important features of these non-covalent interactions is their ability to have concurrent multiple interactions. This synergetic nature often enables these interactions to sustain highly complex (e.g. macromolecules), stable and specific associations. It has been found that the intermolecular non covalent interactions especially involving aromatic rings play vital role in various biological and chemical recognition processes.<sup>3</sup> An excellent example (Fig 1.1) of chemical recognition, involving aromatic system, followed by shape switching has been reported by Lehn and coworkers.<sup>4</sup> The report shows the receptor - substrate recognition and subsequent change in the shape, due to intermolecular p-orbital overlap between two  $\pi$ -conjugated systems

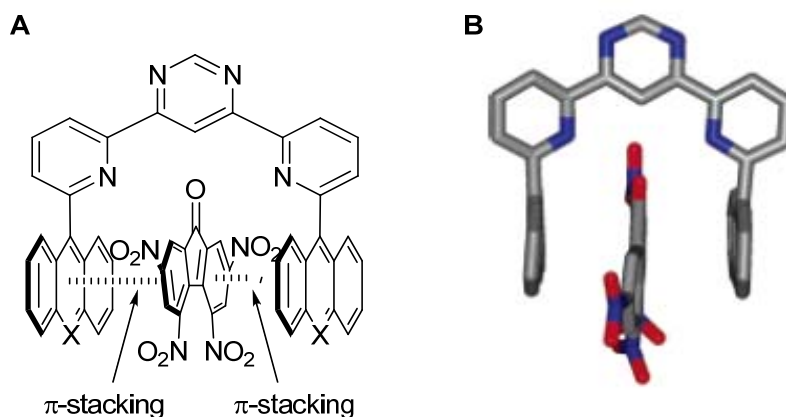


**Figure 1.1:** A) Schematic representation of the  $\pi$ -staging between receptor (with two parallel arms) and substrate (fastened in between arms of the receptor). B) Crystal structure of the assembly.

Another potent interaction between cation and an aromatic system termed as cation- $\pi$  interaction has been widely studied and its nature and energetic are well investigated.<sup>5-8</sup> In the well explored field of cation- $\pi$  interaction, there have been lots of reports of the interaction of cation with  $\pi$ -cloud of aromatic system. This interaction plays a vital role in important biological systems like the binding site of alkylamine dehydrogenase and acetylcholine esterase. Also the natural  $K^+$  channel are well facilitated by cation- $\pi$  interaction. There have been numerous efforts to use this interaction to make synthetic ion channel. A remarkable development reported by Matile *et.al.*<sup>9</sup> present the use of rigid arene system as a  $\pi$ -slide. The reported  $\pi$ -slide system (figure1.2) contains a ligand binding site (EDA, iminodiacetate) and a spacer, and has been used to make first ligand-gated, synthetic  $K^+$  channel. The rigid-rod arene system may serve as a consecutive binding site for the cation.

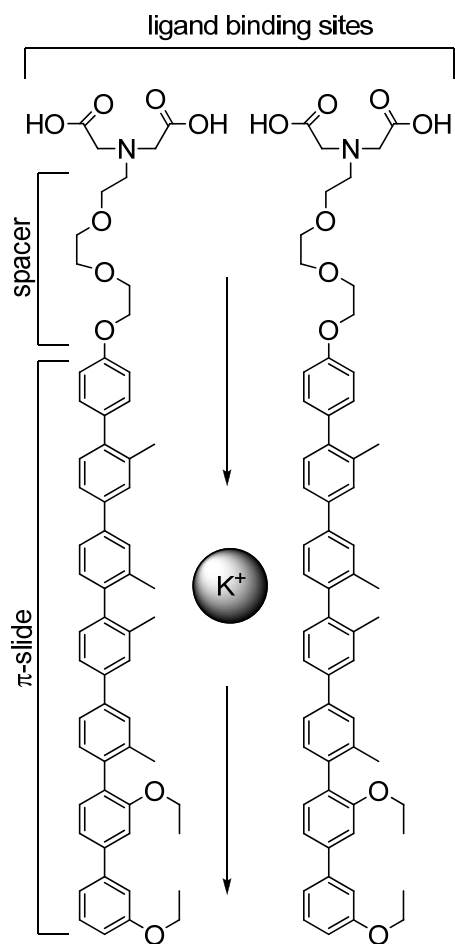


**Figure 1.2:** Construction of the  $K^+$  selective channel through cation- $\pi$  interactions.



Recently a new type of interaction, anion- $\pi$  interaction has attracted considerable attention and eventually has developed in to a new branch of supramolecular chemistry. The sudden growth in this novel area has been driven by a number of reasons. Anions are ubiquitous in biological system. Majority of cofactors and enzymes substrates are anionic in nature and so is the genetic information carrier DNA (a poly anion). Further anion recognition has its application in context of important areas like medicine, catalysis and removal of environmental contaminants.<sup>10</sup>

Typically, an anion- $\pi$  interaction refers to a non-covalent interaction between an electron deficient,  $\pi$ -acidic aromatic system and an anion. Experimentally it was observed, first, in the solid state in  $\text{Cl}^- \dots s$ -triazine complex<sup>11</sup> and in solution in anion- binding studies of N-confused porphyrins<sup>12</sup> as a secondary interaction. Subsequent studies have elegantly shown that the major contribution in anion- $\pi$  interaction comes from electrostatic and anion-induced polarization. The electrostatic component is interrelated to the quadrupole moment ( $Q_{zz}$ ) of the electron deficient aromatic ring. The quadrupole moment of a molecule is the measure of charge distribution relative to a particular molecular axis.<sup>13</sup> In a way quadrupole moment refers to the electron deficiency of the aromatic ring *e.g.* hexafluorobenzene due to attachment of six highly electronegative fluorine atoms, has positive and large quadrupole moment ( $Q_{zz}(\text{C}_6\text{F}_6) = +9.50 \text{ B}$ ;  $1 \text{ B (Buckingham)} = 3.336 \times 10^{-40} \text{ C m}^2$ ) where as for benzene it is large and negative ( $Q_{zz}(\text{C}_6\text{H}_6) = 28.48 \text{ B}$ ).<sup>17</sup>

Though due to its counter intuitive nature and synthetically challenging factors inherent to the anions, area of anion- $\pi$  interaction had till now been overlooked as compared to its more developed counterpart cation- $\pi$  interaction; There are quite of few reports investigating its theoretical aspects as well as experimental evidences. Alkorta *et. al.*<sup>14</sup> performed DFT (Density Functional Theory) and MP2 ab initio calculations on the interactions between several electron deficient aromatic rings, *e.g.*, hexafluorobenzene, octafluoronaphthalene and pentafluoropyridine and the anions  $\text{F}^-$ ,  $\text{Cl}^-$ ,  $\text{Br}^-$ ,  $\text{CN}^-$  and  $\text{CNO}^-$ . The qualitative outcomes of these studies done in each case have revealed a favorable non covalent interaction between the anion and the  $\pi$ - cloud of the aromatic system. Further the first X-ray crystal structures with recognized and explicit anion- $\pi$  interactions were in parallel reported in 2004 by Reedijk *et. al.*<sup>15</sup> and Meyer *et. al.*<sup>20</sup> Reedijk *et. al.* presented a notable supramolecular system involving the dendritic octadentate ligand  $N,N',N'',N'''$ -tetrakis{2,4-bis(di-2-pyridylamino)-1,3,5-triazinyl}-1,4,8,11-

tetraazacyclotetradecane (L1; figure 1.3A) coordinated to Cu(II) chloride to afford the tetranuclear complex  $[\text{Cu}_4(\text{L1})\text{Cl}_4][\text{Cl}]_4(\text{H}_2\text{O})_{13}$  (figure.1.3B). In this complex, 16 pyridyl rings of L1 are coordinated to four different Cu(II) ions, and two  $\text{Cl}^-$  anions are entrapped in the two cavities formed by the pyridyl rings (shortest anion-to-centroid distance 3.012 Å), as well as in close contact to the triazine rings, thus establishing anion- $\pi$  interactions (Figure.1.3B).

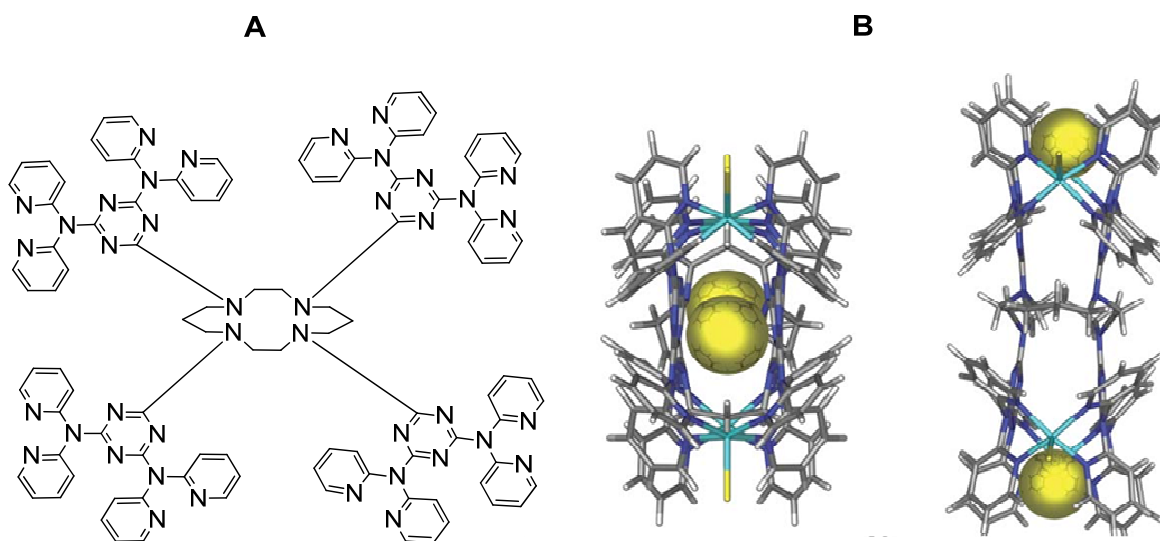


**Figure 1.3:** (A) schematic diagram of *N,N',N'',N'''*-tetrakis{2,4-bis(di-2-pyridylamino)-1,3,5-triazinyl}-1,4,8,11-tetraazacyclotetradecane(L1). (B) Crystal structure of  $[\text{Cu}_4(\text{L1})\text{Cl}_4][\text{Cl}]_4(\text{H}_2\text{O})_{13}$  from two different standpoints. Atom colors: C= grey, H= white, N = dark blue, Cu = light blue and Cl = yellow. Figure adopted from reference 11.

Other than inorganic complexes, there are excellent examples of organic moieties which can be used to entrap anions. Recently reported investigation by Gorteau *et.al.*<sup>16</sup> presents the synthesis and evaluation of  $\pi$ -acidic oligo-(*p*-phenylene)-*N,N*-naphthalenediimide (O-NDI) rods that can transport anions across lipid bilayer membranes with an unusual halide selectivity ( $\text{Cl}^- > \text{F}^- > \text{Br}^- > \text{I}^-$ ). The concept is schematically depicted in the figure 1.4.

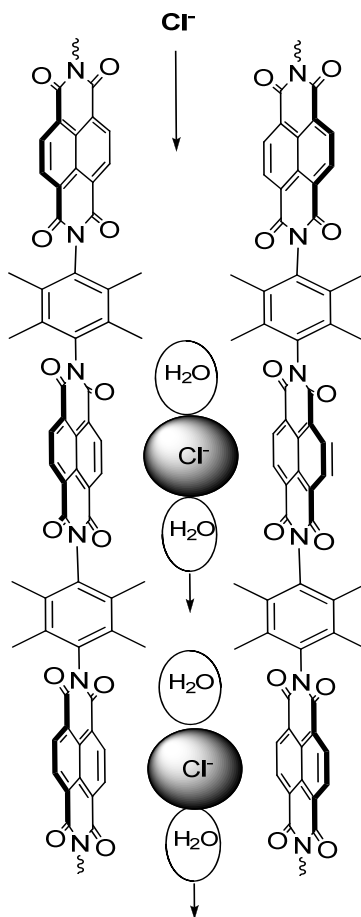


**Figure 1.4:** The concept of anion- $\pi$  slide. Anions are sliding through the tunnel between two  $\pi$ -slides.

Another important example, which provides the evidence of anion- $\pi$  interaction in solution, was reported by Kochi *et. al.*<sup>17</sup> where they have examined a series of neutral organic  $\pi$ -acceptors (e.g. tetracyanopyrazine, tetracyanobenzene etc.) with electron deficient aromatic rings (Fig. 29a) in solution by UV/vis spectroscopy. Addition of the Solutions of the tetraalkylammonium salts of Cl<sup>-</sup>, Br<sup>-</sup>/I<sup>-</sup> slowly with increasing concentration induced the appearance of new peaks which indicates the charge transfer process.



## Chapter 2

### Design:

In the area of supramolecular chemistry, calixarene has been sought after since long time, particularly in context of host-guest chemistry. Features such as easy availability, unique conformational and cavity structure, and recognition properties have made it an obligatory part of supramolecular chemistry. One of the recent developments in this area is the use of heteroatomic rings instead of fundamental phenol unit. This replacement has been used to tune the cavity size and thereby to make it more efficient. Use of triazene, a benzene ring with three nitrogen atom has gained the reputation as a good replacement for phenol rings in calixarene assembly. Triazene has been reported as a valuable moiety in self assembly as well as in molecular recognition. This potency of the triazene is attributed to its capabilities to act as both hydrogen bond donors and acceptors to bind guest molecules such as carbohydrates, cyanuric acid and uracil derivatives through multiple hydrogen bondings.<sup>18</sup> Although triazene moiety has been incorporated in few macrocycles molecules, the assembly of calixarene scaffolds using triazene as the building units has not been explored to the appropriate extent especially in the context of anion sensing. This report presents the synthesis and UV evaluation of an anion sensor (Figure 2.1), a novel derivative of triazene based calixarene (tetraoxocalix[2]arene[2]triazene) with  $\pi$ -acidic *N, N*-naphthalenediimide (NDI) units linked by a spacer.

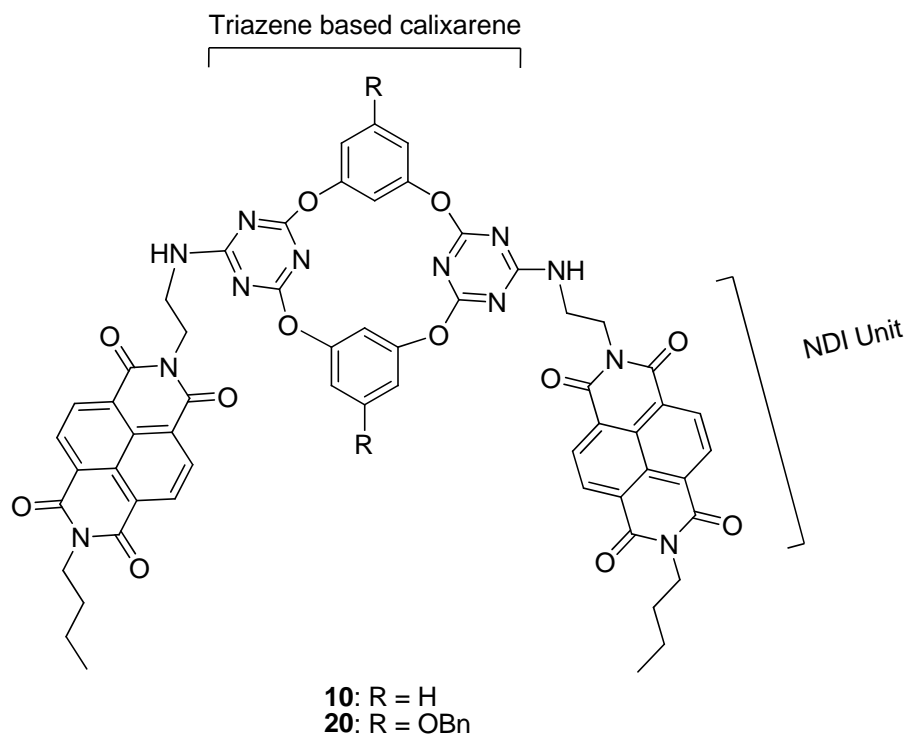


**Figure 2.1:** The schematic diagram of the synthesized structure with different units involved.

Use of NDI unit to serve as an electron deficient aromatic system has been well supported by an earlier report<sup>16</sup> where it has been used as building block of synthetic anion channel and has been described as a compact, organizable, colorizable, and functionalizable organic *n*-semiconductor. By high-level DFT calculations it has also been shown that the NDI unit have a large and positive global quadrupole moment ( $Q_{zz} = +19.4 \text{ B}$ ),<sup>13</sup> which makes it appropriate for the role of electron deficient unit in anion- $\pi$  interaction.

Anion trapping can be sensed by the conformational change which occurs in the system during its interaction with anions. The crystal structure of the triazene based similar Calixarene have been reported by Mei-Xiang *et. al.* (figure 2.2),<sup>19</sup> shows that the two benzene rings are parallel to each other.

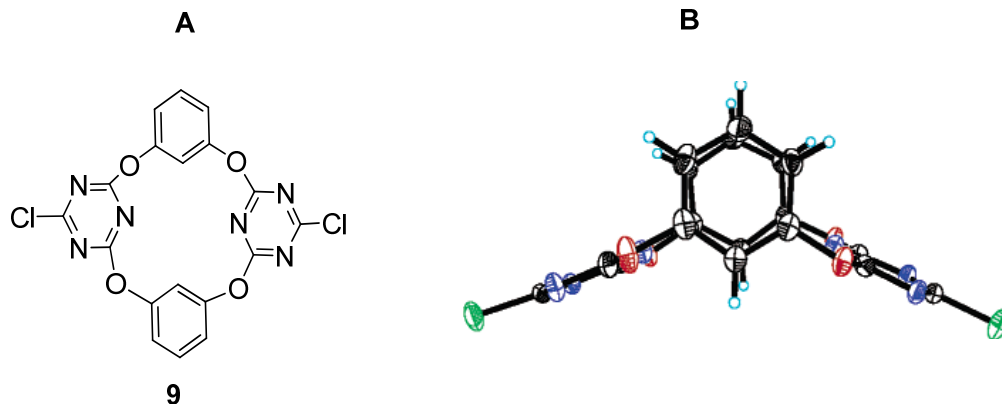


**Figure 2.2:** A) The reported triazene based calixarene. B) Crystal structure of the calixarene which shows two overlapping benzene ring with two substituted triazene ring flanking outwards.

Another report<sup>19</sup> by the same group gives evidence that the substitution in the triazene unit of the above mentioned calixarene results in the change in the conformation of the remaining two benzene rings. Based on these evidences, the proposed structure is expected to change the conformation (figure 2.3).

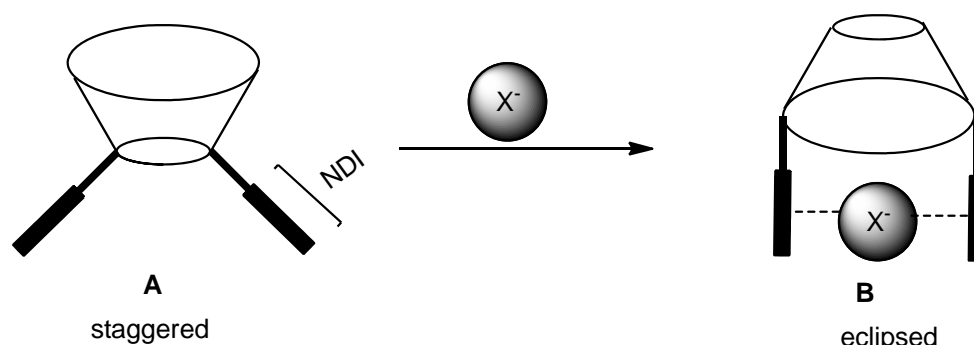


**Figure 2.3:** A) Proposed concept of the anion- $\pi$  interaction where bucket represents the calixarene part where as the NDI part is being depicted by rectangular shaped structure. B) Expected conformation after anion (black sphere) trapping.

The conformational change upon anion binding would result in the change in charge distribution over the different parts of the molecule which can be sensed by different spectroscopic methods like NMR (the chemical shift of peaks *i.e*  $\delta$ , is expected to change) and UV pattern. This report presents the UV study of the synthesized anion sensor which shows the change in UV profile (of appearance of a new peak) with gradual increment in the anion concentration. The change in UV profile provides the proof of the anion- $\pi$  interaction between anions and synthesized molecule.



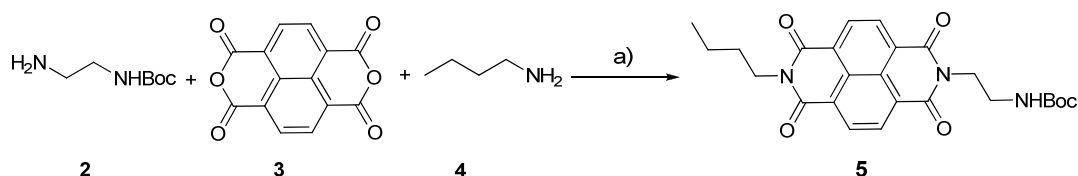


## Chapter 3

### Result and discussion:

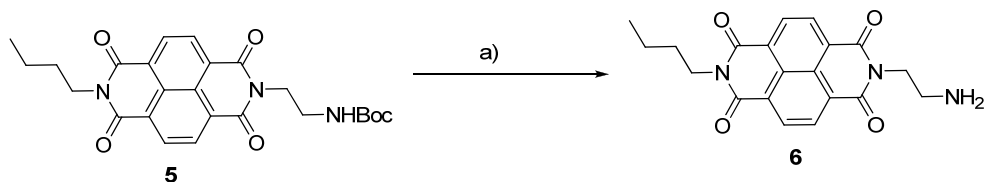
#### 3.1 Synthetic Schemes:

As it is mentioned in the chapter 2, synthesis of the targeted molecule (compound **10**) was started with the synthesis of compound **5** according to scheme given below. A substitution reaction was executed in the presence of base where *n*-butylamine and mono protected ethylenediamine were used as nucleophiles.



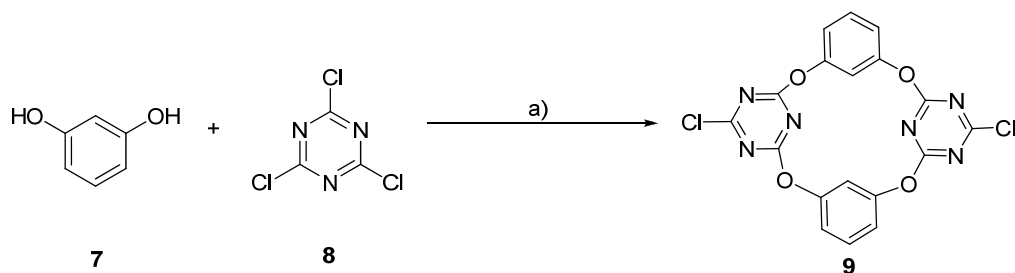
**Scheme 1:** Reagents and conditions: a) TEA, THF, 40 °C, 48 h, 40%

The second step was the deprotection of the compound **5** which was done using trifluoroacetic acid and further neutralization by 10% sodium bicarbonate solution to get compound **6**.



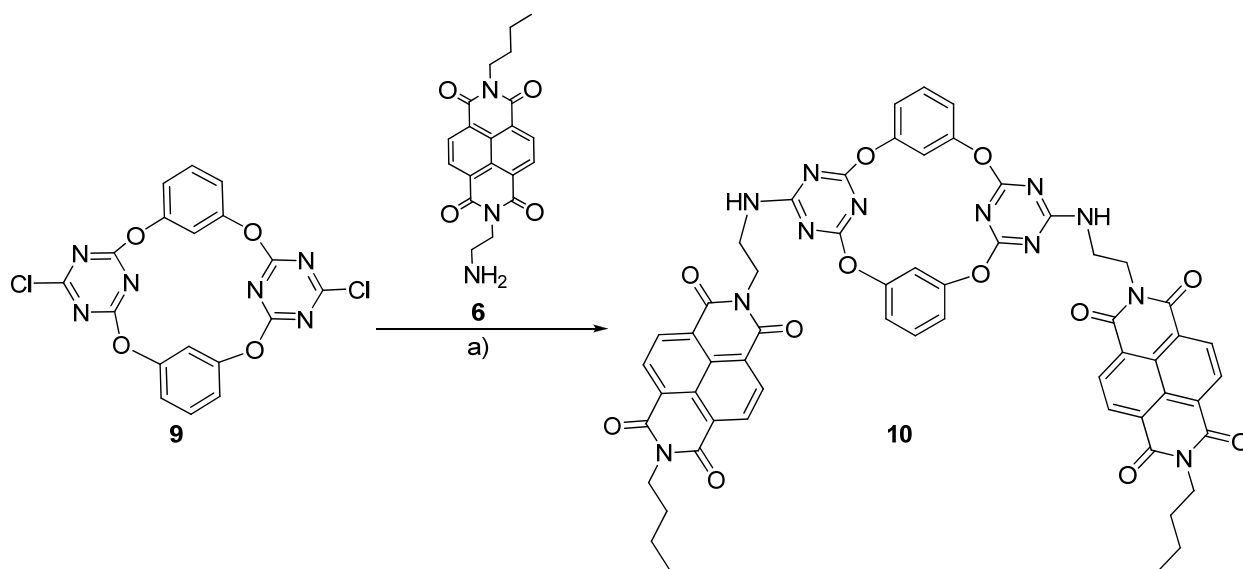
**Scheme 2:** Reagents and conditions: a) TFA, DCM, 0 °C - rt, 2 h, 89%.

Synthesis of triazene based ring was done (Scheme 3) using resorcinol (compound **7**) and cyanuric chloride (compound **8**). Addition of two equivalents of cyanuric chloride and 1 equivalent of resorcinol to a basic solution resulted in an intermediate formation. A trimer with two cyanuric chloride units and one resorcinol unit was formed which was filtered and again added to the basic solution simultaneously with another equivalent of resorcinol to get compound **9**.



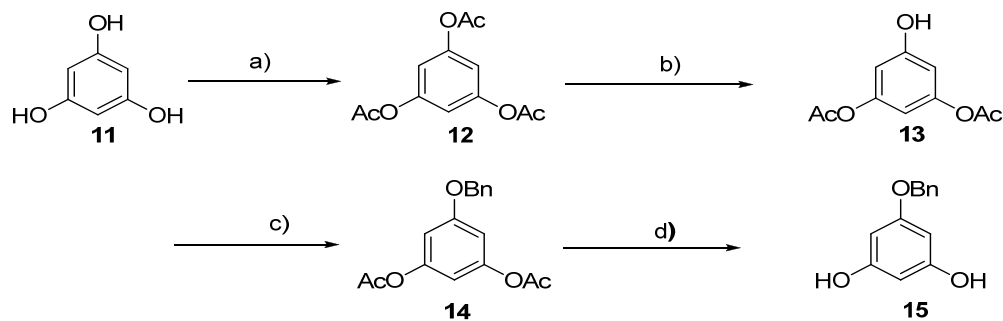
**Scheme 3:** Reagents and conditions: a) DIPEA, THF, rt, 36 h, 12 %

Compound **10** was synthesized via substitution reaction. Two nucleophilic substitutions of chloride units of compound **9** with two units of compound **6** in a basic environment produced **10**.



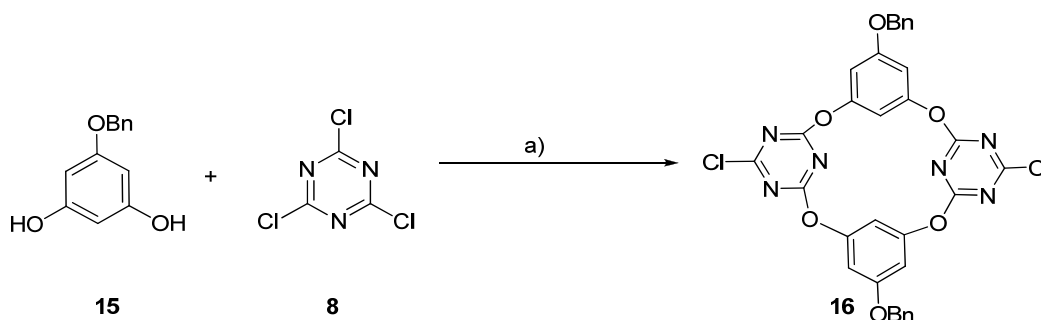
**Scheme 4:** Reagents and conditions: a) DIPEA, DMF, 80 °C, 40 h, 15%

Synthesis of another derivative compound **20** of the compound **10** was executed by taking Phloroglucinol as a precursor to synthesize compound **15** which was further used to synthesize a derivatized form of compound **9**.



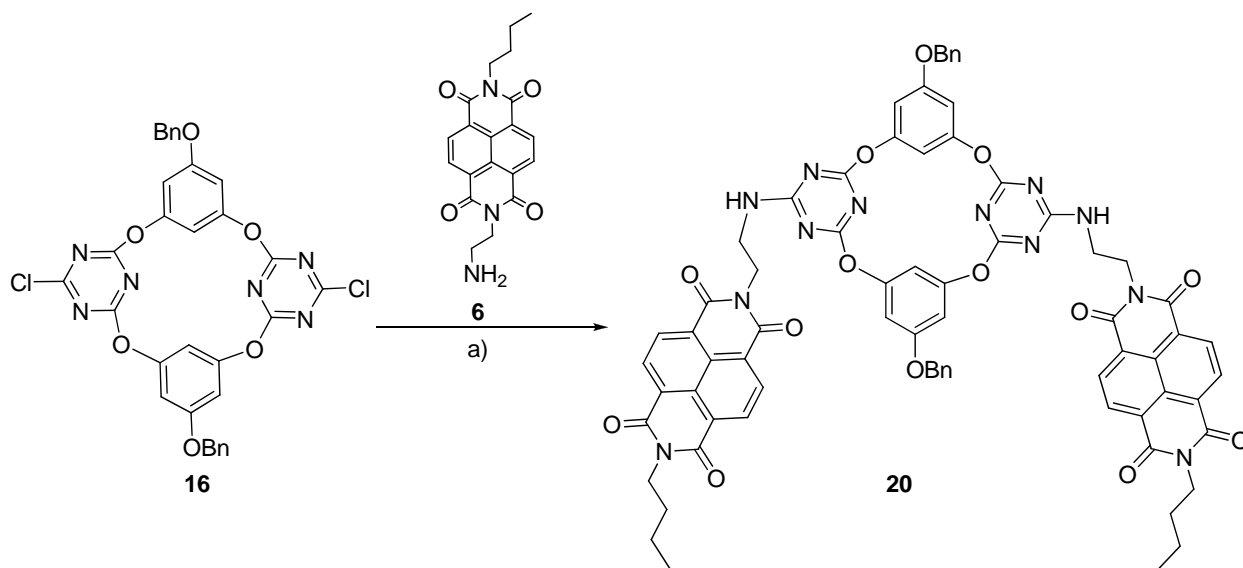
**Scheme 5:** Reagents and conditions: a)  $(\text{Ac})_2\text{O}$ , pyridine, rt, overnight, 82%; b)  $\text{NaBH}_4$ ,  $\text{CoCl}_2 \cdot 6\text{H}_2\text{O}$ , EtOH,  $0^\circ\text{C}$  - rt, 3 h, 80%; c)  $\text{BnBr}$ ,  $\text{K}_2\text{CO}_3$ , DMF,  $-13^\circ\text{C}$ , 6 h, 70%; d)  $\text{K}_2\text{CO}_3$ , MeOH, rt, 86%.

The synthesis of compound **15** could have been carried out by the mono protection of the benzene- 1,3,5-triol but there might be a problem in purification due comparative polarities of the other products like di-protected and tri-protected ones. To avoid this problem a relatively long but efficient route has been followed (scheme 5). Further cyclization to get compound **9** was carried out with cyanuric chloride according to the following scheme.



**Scheme 6:** Reagents and conditions: a) DIPEA, THF (dry), rt, 36 h, 15%.

Finally compound **20** was synthesized by substituting two chloride units of compound **16** by two units of compound **6** in presence of DIPEA.



**Scheme 7:** Reagents and conditions: a) DIPEA, DMF,  $80^\circ\text{C}$ , 40 h, 18%.

### 3.2 Ultra Violet Spectroscopic Studies

After verification of identity and purity of **10** by NMR and MALDI, the UV study of the compound was conducted. The UV profile of **10** was recorded at different concentrations and an appropriate concentration (6 $\mu$ M) where the absorbances of the peaks were about 0.5 was selected. Figure 6.1 represents the UV plot of the targeted NDI compound **10**.

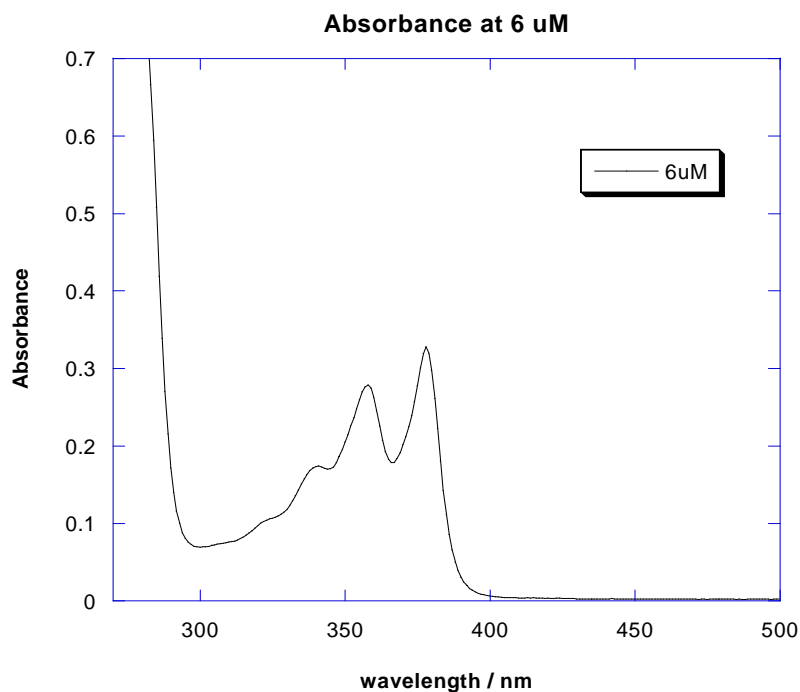


**Figure 3.1:** The absorbance vs. wavelength plot, at 6 $\mu$ M in 9:1 mixture of Acetonitrile / Chloroform. There are two major peaks with higher absorption at 357 nm and 378 nm.

#### Molar absorptivity ( $\epsilon$ ) calculation:

Molar absorptivity ( $\epsilon$ ) or molar extinction co-efficient is the intrinsic property of the compound, a measurement of how strongly a chemical compound absorbs light at a given wavelength. The molar absorptivity can be calculated by using Beer's law which establishes it's relation with concentration(C) and the path length (l) covered by the monochromatic light.

$$A = \epsilon .C. l \quad (\text{Eq. 1})$$

The absorbance at various concentrations has been plotted at wavelength ( $\lambda$ ) 357 nm (plot 2) and 378 nm (plot 3) separately. As path length is constant (cuvette width) the relation yielded a straight line with molar absorptivity as the slope.

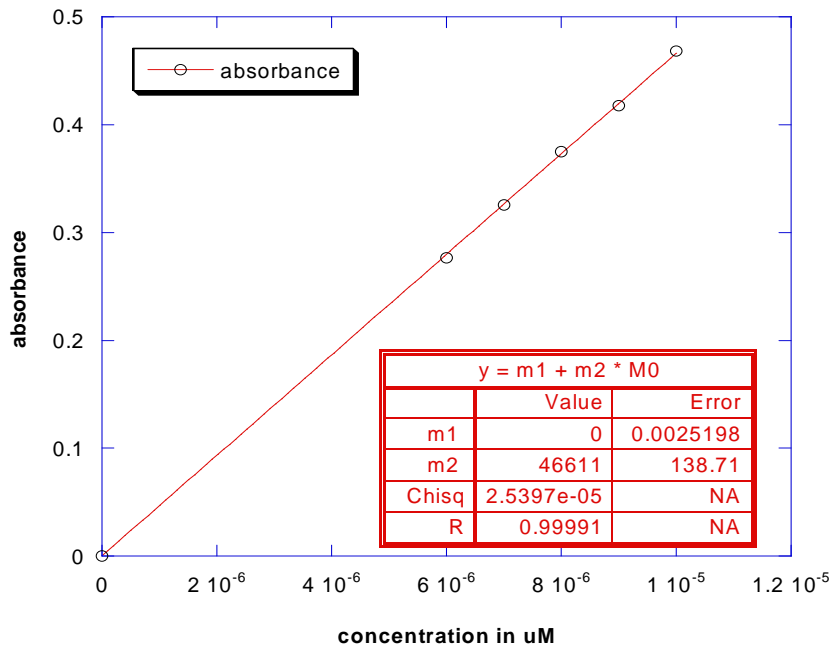


Figure 3.2: Absorbance vs. concentration plot at  $\lambda = 357$  nm.

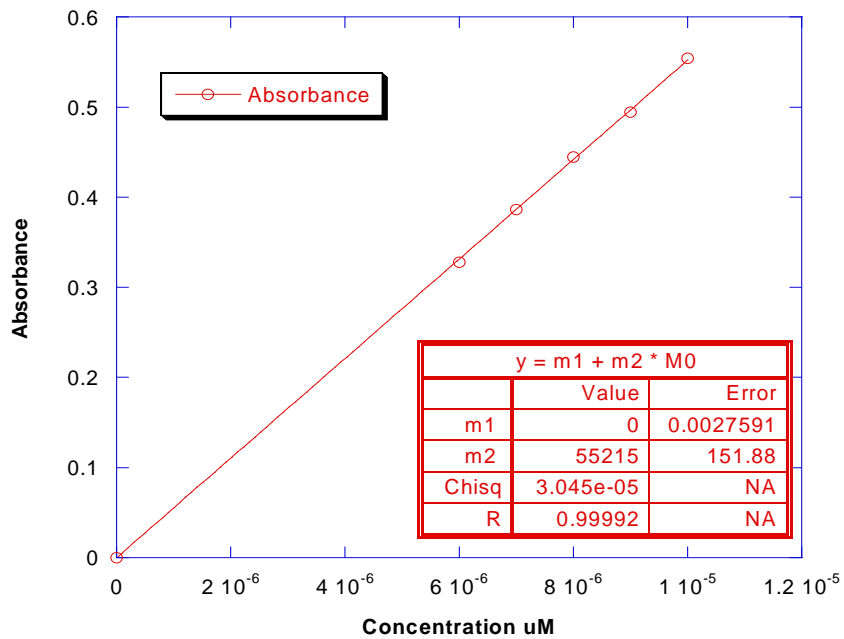
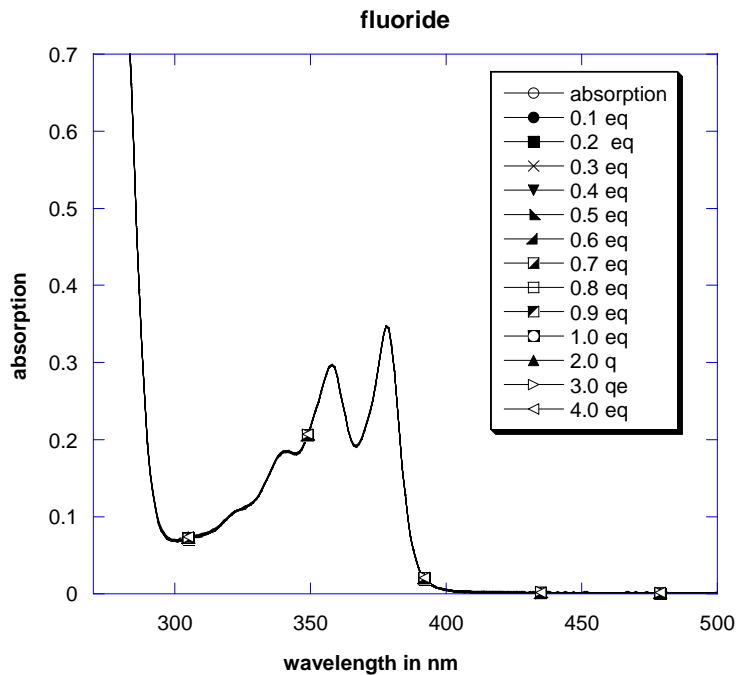


Figure 3.3: Absorbance vs. concentration plot at  $\lambda = 378$  nm.

The high value of the molar absorptivity in both cases is attributed to the highly conjugated structure of the compound. The relatively higher concentration at  $\lambda = 378$  nm as compare to  $\lambda = 357$  is due to higher absorption at  $\lambda = 378$  nm which is apparent from the plot 1.

### Low concentration study:

UV study has been used as a probe to sense the interaction between different anions and the compound (electron deficient  $\pi$  system). Solution of tetrabutylammonium salts of  $F^-$ ,  $Br^-$ ,  $I^-$  were slowly added (from 0.1 equivalent to 4 equivalent) to the  $6 \mu\text{M}$  solution of the compound. At each addition the UV absorption spectra was recorded.



**Figure 3.4:** Absorbance vs. Wavelength plot, at different concentration of the tetrabutylammonium Fluoride (TBAF).

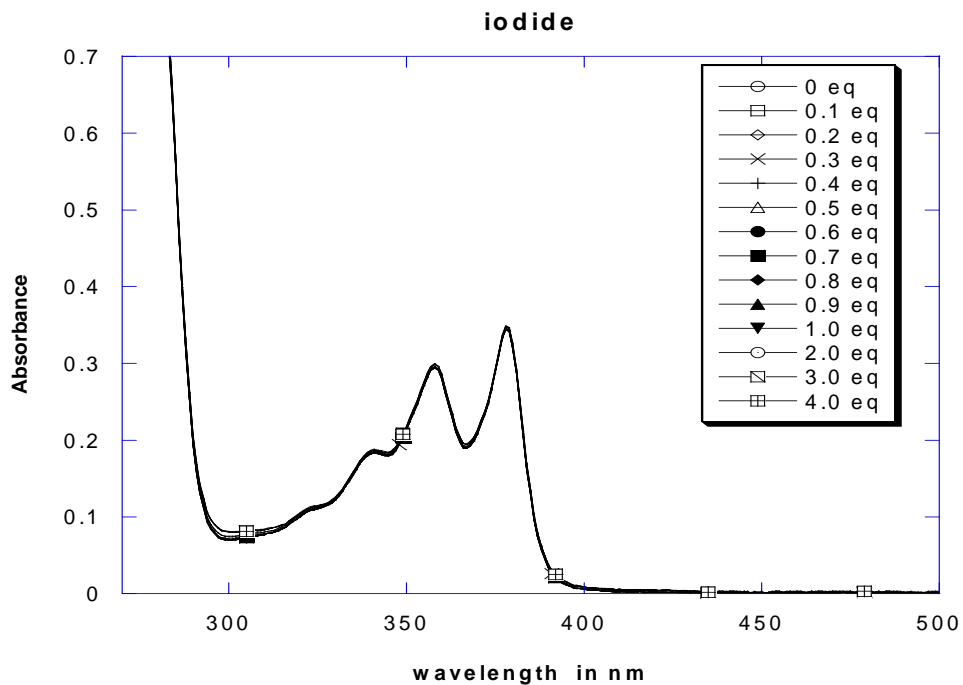
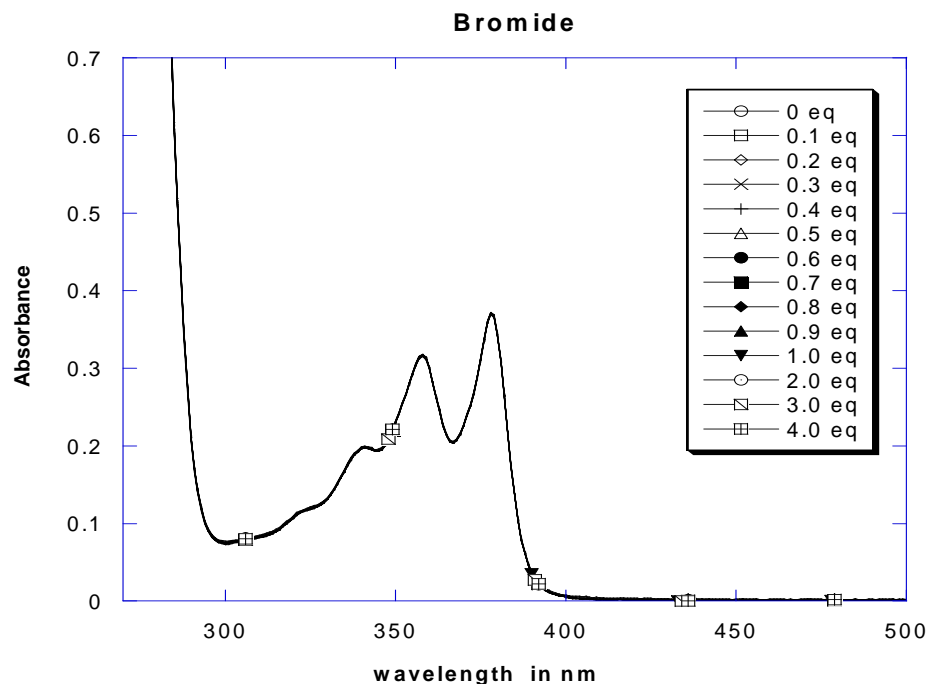


**Figure 3.5:** Absorbance vs wavelength graph at different concentrations of TBA salts Bromide (above) Iodide (below).

As the plots depict for all the anions the UV plot is not showing a difference by changing their concentrations. This implies that at these concentrations the expected anion- $\pi$  interaction between anions and the compound do not exist.

### High concentration study:

Further it was planned to check the anion- $\pi$  interaction at higher concentration. Salts proportion was increased by hundred folds and UV plot was taken by keeping the compound **10** concentrations constant. The figure 6.6 presents the UV plot with Fluoride salt.

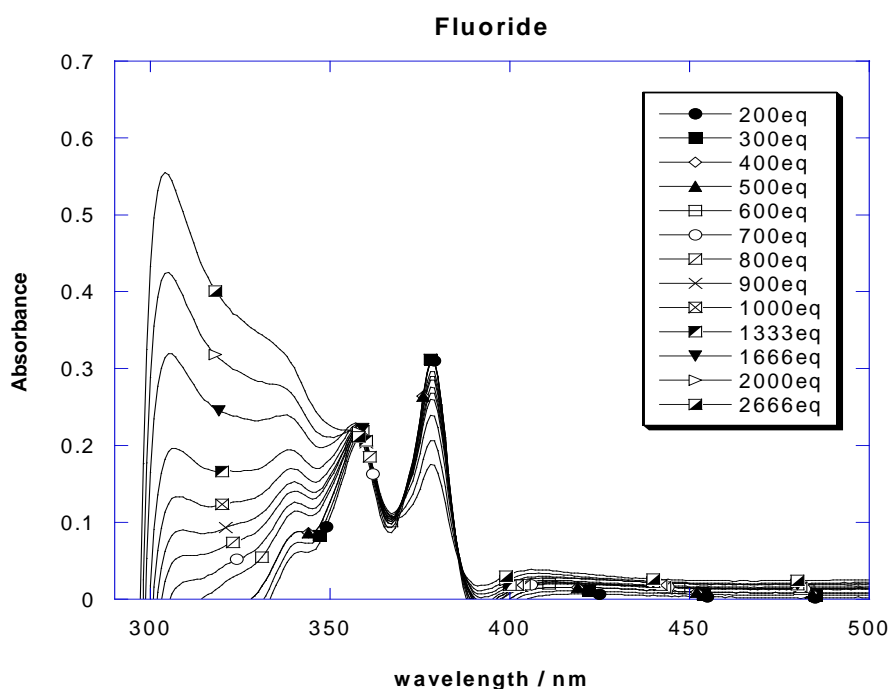


**Figure 3.6:** Absorbance vs. wavelength plot at higher anion concentration of TBAF. table represents the equivalent of salt with respect to compound °C.

The figure 6.6 shows that the gradual increment in the anion concentration induces a new peak around 300 nm whereas the peak at 378 nm is gradually decreasing. This study indicates the existence of the expected anion- $\pi$  interaction between fluoride ion and the synthesized model compound **10**. The plots of consecutive studies done on bromide and iodide anions are given below. From the plots it is evident that these anions are not interacting with the model compound.



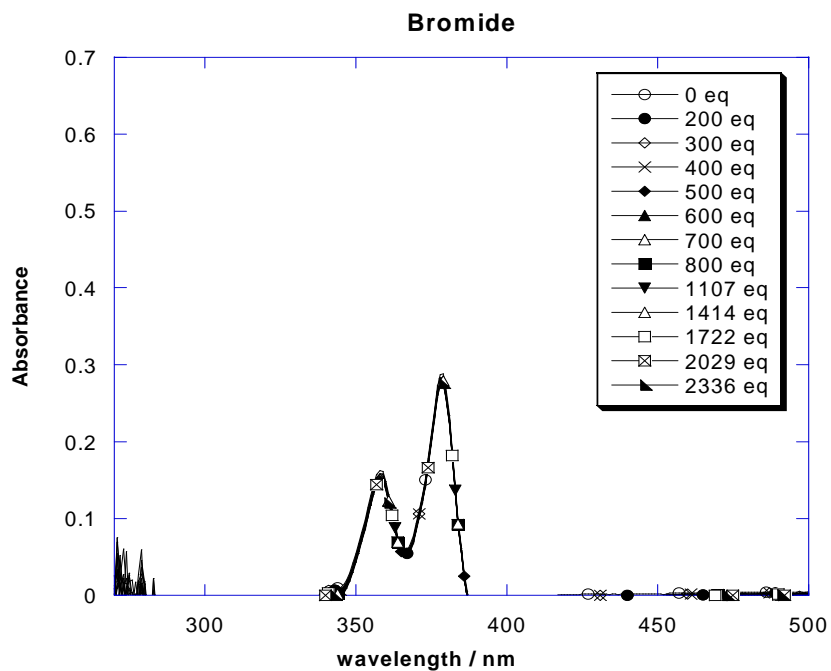


**Figure 3.7:** Absorbance vs. wavelength graph of the solution containing model compound **10** and bromide salt at different salt concentrations.

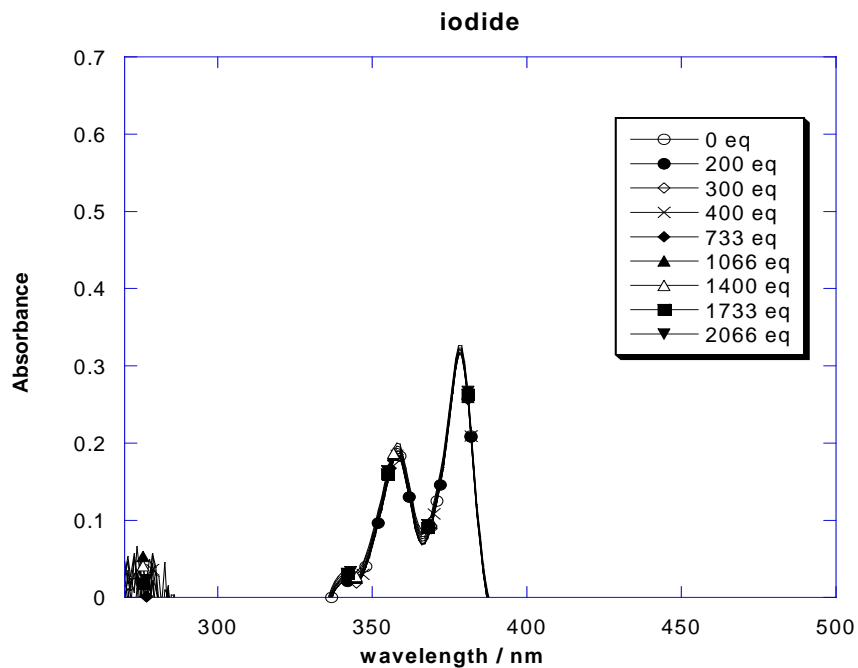
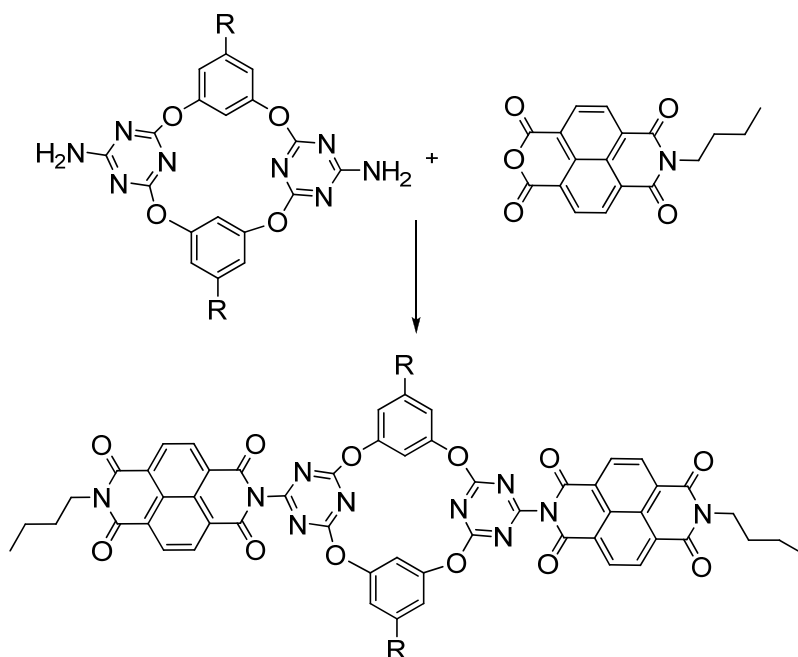


**Figure 3.8:** Absorbance vs. wavelength graph of the solution of iodide salt and compound **10** at different salt concentrations.

The negative UV responses by compound **10** in the bromide and iodide cases and the positive one in the case of the fluoride gives the notion of selectivity, which is an important quality of the anion sensors.

### 3.3 Future prospect:

The synthesis of the novel anion sensor and the studies done in this report gives an idea that the NDI derivative of triazene based Calixarene can be used as a selective anion sensor. The fertile nature of both units involved the Calixarene and the NDI part opens up new possibilities in the contest of tuning the selectivity and its sensitivity. In this direction as an example, a new molecule can be synthesized by removing or changing the spacer connecting these two moieties. The scheme below presents the new molecule without spacer.

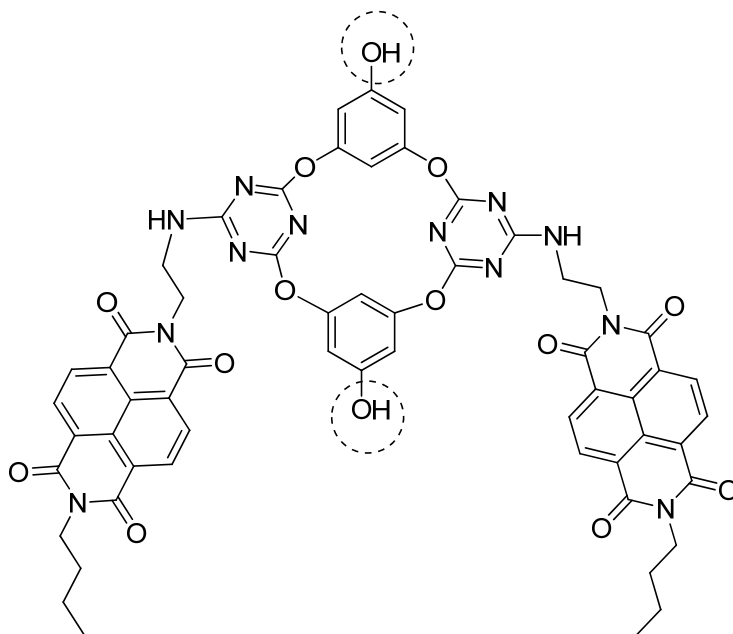


**Scheme 8:** Design of the proposed molecule

From the above mentioned molecule it is expected that this model will show greater distortion there by more sensitivity in the presence of anions which is expected to become apparent in the UV and other spectroscopic studies.

The other major issue with these types of macrocycles is the solubility in polar solvents. The solubility in polar solvents like water is important for biological studies where there are lots

of processes like substrate recognition in enzyme substrate system and ion channels, where anion recognition plays a major role. To increase the solubility some polar group might be attached on various unit involved in the assembly. One step in this direction would be substitution of  $-OH$  group on the calixarene unit. Attachment of the hydroxyl group is expected to increase the solubility of the molecule by increasing the chance of hydrogen bonding. This scheme (final product is given below) also has been partly pursued and synthesis of the intermediate (compound 16) is given in the synthesis part of the scheme.



**Scheme 9:** Compound, with substitutions on the benzene ring of the calixarene unit to improve its solubility.

The ease with which new derivatives can be synthesized from the model compound and its potential applications in various fields like biology and environmental contaminant removal, it opens up the new and promising horizon in the field of anion recognition.



## Chapter 4

### Experimental Section

#### 4.1 Materials and methods:

All reactions were conducted under the nitrogen atmosphere. All the chemicals were purchased from commercial sources and used as received unless stated otherwise. Solvents: petroleum ether and ethyl acetate (EtOAc) were distilled prior to thin layer and column chromatography. THF was pre-dried over Na wire. Then the solvent was refluxed over Na (1% w/v) and benzophenone (0.2% w/v) under an inert atmosphere until the blue color of the benzophenone ketyl radical anion persists. *N,N*-Dimethylformamide (DMF) was pre-dried over calcium hydride and then distilled under vacuum. Column chromatography was performed on Merck silica gel (100–200 mesh). TLC was carried out with E. Merck silica gel 60-F-254 plates.

#### 4.2 Instrumentations:

The  $^1\text{H}$  and  $^{13}\text{C}$  spectra were recorded on 400 MHz Jeol ECS-400 (or 100 MHz for  $^{13}\text{C}$ ) spectrometers using either residual solvent signals as an internal reference or from internal tetramethylsilane on the  $\delta$  scale ( $\text{CDCl}_3$   $\delta_{\text{H}}$ , 7.24 ppm,  $\delta_{\text{C}}$  77.0 ppm). The chemical shifts ( $\delta$ ) are reported in ppm and coupling constants ( $J$ ) in Hz. The following abbreviations are used: m (multiplet), s (singlet), br s (broad singlet), d (doublet), t (triplet) dd (doublet of doublet). High-resolution mass spectra were obtained from Shimadzu, GC-2010 Gas Chromatography-Mass Spectrometer. High-resolution mass spectra were obtained from MicroMass ESI-TOF MS spectrometer. Absorption spectra were recorded on a PerkinElmer, Lambda 45 UV-Vis spectrophotometer. (FT-IR) spectra were obtained using NICOLET 6700 FT-IR spectrophotometer as KBr disc and reported in  $\text{cm}^{-1}$ . Melting points were measured using a VEEGO Melting point apparatus. All melting points were measured in open glass capillary and values are uncorrected. Crystal structures were recorded on a Bruker single crystal X-Ray diffractometer. Geometry optimizations were carried out at MM2 level of theory using the program ChemBio3D Ultra 12.0.

### 4.3 Synthetic procedures:

**Compound 2.** To the solution of **1** (11.2 ml, 167.7 mmol) in 50 ml DCM at 0 °C, was added the solution of (Boc)<sub>2</sub>O (6.4 ml, 28 mmol) in 400 ml of DCM for 6 hours. After addition, reaction mixture was stirred overnight at rt. The reaction mixture was washed with water (25 ml x 3) and brine (25 ml x 2), passed over Na<sub>2</sub>SO<sub>4</sub> and dried over vacuum. Column chromatography of crude product (CHCl<sub>3</sub> / MeOH 93/7) yielded **2** (4.2 g, 93%) as viscous colorless liquid. TLC (DCM / MeOH 1/5): R<sub>f</sub> 0.47; <sup>1</sup>H NMR (400 MHz, CDCl<sub>3</sub>): δ ppm 7.92 (br s, 1H), 5.19 (br s, 2H), 3.11-3.05 (m, 2H), 2.72-2.68 (m, 2H), 1.34 (s, 9H); <sup>13</sup>C NMR (100 MHz, CDCl<sub>3</sub>): δ ppm 156.33, 79.07, 43.26, 41.79, 28.41.

**Compound 5.** To the solution of **4** (32.67 mg, 0.448 mmol) in dry DMF (5 ml), **2** (103 mg, 0.448 mmol), **3** (100 mg, 0.373 mmol) and TEA (0.25 ml, 1.12 mmol) were added. The reaction mixture was stirred at 40 °C for 24 h. After evaporation of solvent under reduced pressure, crude product was purified by column chromatography (EA / PE 15/85) to afford **5** (76 mg, 38%) as pinkish solid. TLC (EA / PE 1/2): R<sub>f</sub> 0.61; mp: 199-200 °C; IR: 3354 (m), 2968 (w), 1704 (m), 1686 (m), 1655 (s), 1578 (s), 1532 (m), 1453 (s), 1369 (w), 1348 (w), 1288 (s), 1186 (m), 1165 (w), 1081 (w), 1070 (w); <sup>1</sup>H NMR (400 MHz, CDCl<sub>3</sub>): δ ppm 8.75 (s, 4H), 4.83 (s, 1H), 4.37 (t, *J* = 4 Hz, 2H), 4.19 (t, *J* = 8 Hz, 2H), 3.57-3.53 (m, 2H), 1.76-1.68 (m, 2H), 1.49-1.42 (m, 2H), 1.2 (s, 9H), 0.98 (t, *J* = 8 Hz, 3H); <sup>13</sup>C NMR (100 MHz, CDCl<sub>3</sub>): δ ppm 163.29, 162.89, 156.22, 131.14, 130.98, 40.85, 40.71, 39.25, 30.22, 28.22, 20.42, 13.89; MS (MALDI TOF, CHCl<sub>3</sub>): m/z 504.1438 [M + K]<sup>+</sup>.

**Compound 6.** To an ice cooled solution of **5** (400 mg, 0.860 mmol) in DCM (2 ml), TFA (1 ml in 2 ml DCM) was added dropwise. The reaction was stirred at rt for 1 hr. After completion the reaction was taken in to the 30 ml of ethyl acetate and NaHCO<sub>3</sub> solution (10 %) was added to make it basic (pH=8-9) which resulted in pinkish precipitate. Filtration followed by water wash yielded pink solid **6** (280 mg, 89%). TLC (MeOH/ CHCl<sub>3</sub> 1/10): R<sub>f</sub> 0.35; mp: 180-181 °C; IR: 3451 (m), 1703 (m), 1659 (s), 1578 (s), 1416 (m), 1339 (m), 1251 (s), 1210 (w), 1184 (w),

928(w). <sup>1</sup>H NMR (400 MHz, DMSO): δ ppm 8.67 (s, 4H), 7.75 (s, 2H), 4.27 (s, 2H), 4.01 (s, 2H), 3.28(s, 2H), 3.12 (s, 2H), 2.45 (s, 2H), 1.60(s, 2H), 1.33(s, 2H) 0.89-0.90 (m, 3H); <sup>13</sup>C NMR (100 MHz, DMSO): δ ppm 173.36, 170.77, 160.69, 152.02, 135.52, 128.88, 127.70, 107.40, 107.01, 70.96, 29.78 MS (MALDI TOF, CHCl<sub>3</sub>): m/z 365.1476[ M ]<sup>+</sup> .

**Compound 9.** To an ice-cold solution of **8** (5.55 g, 30 mmol) in 60 ml THF, a mixture of **7** (1.65 g, 15 mmol) and DIPEA (4.48 g, 37.5 mmol) in 60 ml THF was added for 2 h. The reaction mixture was stirred for 2 h at rt followed by filtration. The filtrate and **7** (1.3 g in 120 ml THF) were added simultaneously to solution of DIPEA for 3 h .The reaction was allowed for next 36 hr. After removal of the solvent, residue was subjected to column chromatography using 100-200 mesh silica gel with 8 % EA/ PE system to get pure **9** as white crystal. Yield: 25 %; TLC (EA/ PE 3/10): R<sub>f</sub>0.74; mp > 300 °C; IR: 1557 (s), 1440 (m), 1387 (s). <sup>1</sup>H NMR (400 MHz, DMSO): δ ppm 7.29 (t, J = 8 Hz, 2H), 6.88-6.82 (m, 4H), 6.68 (t, J= 4 Hz ,2H); <sup>13</sup>C NMR (100 MHz, DMSO): δ ppm 174.62, 172.55, 151.67, 130.91, 119.58, 116.02; MS (MALDI TOF, CHCl<sub>3</sub>): m/z 466.1580[ M + Na ]<sup>+</sup> .

**Compound 10.** To a solution of **9** (50 mg, 0.113 mmol) in DMF (2 ml) were added compound **6** (82 mg, 0.237 mmol) and DIPEA (38μL, 0.237 mmol). Reaction Mixture was stirred at 80 °C for 25 hr, solvent was evaporated and purification was done by silica gel (100-200 mesh) column chromatography with CHCl<sub>3</sub> as eluent to get **10** (35 mg, 28 %) as pink solid. TLC ( MeOH/ CHCl<sub>3</sub> 1/20 ) R<sub>f</sub>: 0.7; mp: 228-229 °C; IR: 3413 (s, br), 2363 (w), 2343 (w), 1706 (m), 1664 (m), 1578 (s), 1419 (m), 1333 (w), 1247 (w), 1174 (w); <sup>1</sup>H NMR (400 MHz, CDCl<sub>3</sub>): δ ppm 8.72 (d, j= 4 Hz, 8H), 7.08 (t, J = 8 Hz, 2H), 6.68 (d, J = 8 Hz, 2H), 6.64- 6.53 (m, 4H); 6.38-6.35 (m, 2H), 4.55 (t, J = 4 Hz, 4H), 4.18 ( t, J = 8 Hz, 4H), 3.96 – 3.89 (m, 2H), 1.75-1.67 (m, 4H), 1.49-1.40 (m, 4H), 0.97 (t, J = 8 Hz, 6H); MS (MALDI TOF, CHCl<sub>3</sub>): m/z 1101 [M]<sup>+</sup>, 1123.5533[ M + Na ]<sup>+</sup> .

**Compound12.** To a solution of **11** (2.56 g, 20 mmol) in 10 ml pyridine, drop wise addition of acetic anhydride (9 ml, 100 mmol) was done at rt. After stirring for 30 h, the reaction mixture was taken in to 30 ml of DCM and subsequently washed with water (15 ml x 3), 1N HCl (20 ml

x 3) and brine (20 ml x 1) respectively. Solvent was evaporated under reduced pressure to afford pure **12** (4.3 g, 82%) as a white solid. TLC (EA / PE 1/1):  $R_f$  0.62; mp: 102-103 °C; IR: 3091 (w), 1765 (s), 1601 (m), 1457 (w), 1367 (m), 1189 (s), 1123 (s), 1023 (s), 985 (w), 918 (m), 842 (w), 670 (m).  $^1\text{H}$  NMR (400 MHz,  $\text{CDCl}_3$ ):  $\delta$  ppm 6.82 (s, 3H), 2.26 (s, 9H);  $^{13}\text{C}$  NMR (100 MHz,  $\text{CDCl}_3$ ):  $\delta$  ppm 168.67, 151.16, 112.86, 21.16; MS (MALDI TOF,  $\text{CHCl}_3$ ):  $m/z$  291.0241 [M + K] $^+$ .

**Compound 13.** To a solution of **12** (1.5 g, 5.95 mmol) in distilled ethanol (50 ml) was added  $\text{CoCl}_2 \cdot 6\text{H}_2\text{O}$  (14 mg, 1 mol %). The reaction mixture was stirred for 30 min and then cooled to 0 °C,  $\text{NaBH}_4$  (900 mg, 23.75 mmol) was added and reaction was further stirred for next 6 h at 0 °C. After completion of the reaction (monitored by TLC), it was diluted with 100 ml water/ ethyl acetate (1:1) mixture. The organic layer was separated, washed with brine (2 x 20 ml), dried over  $\text{Na}_2\text{SO}_4$  and concentrated under reduced pressure. Crude was purified by column chromatography using silica gel (100-200 mesh) and MeOH /  $\text{CHCl}_3$  (1/ 50) as eluent to get pure **13** (900mg, 72%). TLC ( $\text{CHCl}_3$  / MeOH 10/1):  $R_f$  0.48; mp: 110-111 °C; IR: 3359 (s), 2361 (w), 1752 (s), 1727 (s), 1467 (m), 1439 (s), 1376 (m), 1239 (m), 1215 (s), 1144 (m), 1118 (m), 1029 (w), 920 (w), 894 (m);  $^1\text{H}$  NMR (400 MHz,  $\text{CDCl}_3$ ):  $\delta$  ppm 6.24 (s, 3H), 5.14 (d,  $J = 2.37$  Hz, 1H), 0.99 (s, 6H);  $^{13}\text{C}$  NMR (100 MHz,  $\text{CDCl}_3$ ):  $\delta$  ppm 192.70, 177.18, 170.02, 114.74, 114.51, 76.60; MS (MALDI TOF,  $\text{CHCl}_3$ ):  $m/z$  249.0002 [M + K] $^+$ .

**Compound 14.** A solution of **13** (100mg, 0.5mmol) was prepared in 3ml dry DMF and cooled to -13 °C. Addition of  $\text{K}_2\text{CO}_3$  (140 mg, 1 mmol) and Benzyl bromide (67  $\mu\text{L}$ ) was done in order, and reaction was stirred for 6 h at the same temp. After completion, the reaction was taken in to chloroform (50 ml), washed with water (2x 20 ml) and brine (2x15 ml), dried over  $\text{Na}_2\text{SO}_4$  and concentrated under reduced pressure. Column purification of the residue using silica gel (100-200 mesh) with EA/ PE (8 %) yielded white solid **14** (100 mg, 70%). TLC ( EA/ PE 30/ 100):  $R_f$  0.51; mp: 102-103 °C; IR  $\nu$  3435 (w), 2933 (w), 1774 ( s), 1607 (s), 1461 (m), 1375 (m), 1197 (s), 1139 (s), 1030 (m), 897 (w);  $^1\text{H}$  NMR (400 MHz,  $\text{CDCl}_3$ ):  $\delta$  ppm 7.39-7.37 (m, 6H), 6.61 (d,  $J = 2.39$  Hz, 2H), 6.52 (t,  $J = 2.34$  Hz, 1H), 4.99 (s, 2H), 2.25 (s, 6H);  $^{13}\text{C}$  NMR (100 MHz,



CDCl<sub>3</sub>):  $\delta$  ppm 168.90, 159.82, 136.08, 128.6, 128.16, 127.54, 108.06, 106.11, 70.38, 21.09; MS (MALDI TOF, CHCl<sub>3</sub>): m/z 291.3321[M + K]<sup>+</sup>.

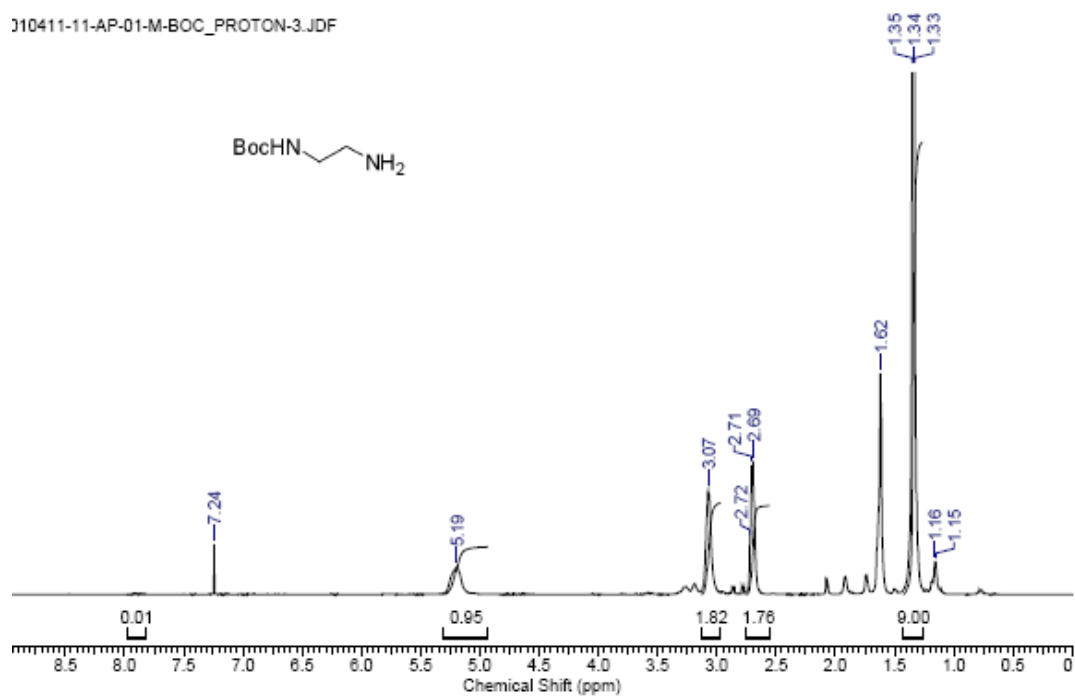
**Compound 15.** To a solution of **14** (100 mg, 0.33 mmol) in MeOH (10 ml), K<sub>2</sub>CO<sub>3</sub> (250 mg) was added and reaction was stirred at rt for 2h. After completion solvent was evaporated and residue was purified by column chromatography using silica gel (100- 200 mesh) with 3% MeOH/ CHCl<sub>3</sub> as an eluent to get golden colored solid **15** ( 62 mg, 86%). TLC (10 % MeOH/ CHCl<sub>3</sub>): R<sub>f</sub> 0.55; mp: 90-91 °C; IR  $\nu$  3345 (s, b), 3034 (w), 1621 (s), 1499 (s), 1485 (s), 1454 (m), 1385 (m), 1365 (m), 1159 (s), 1052 (m), 968 (m), 818 (s); <sup>1</sup>H NMR (400 MHz, CD<sub>3</sub>):  $\delta$  ppm 7.32-7.36 (m, 5H), 5.92 (d, *J* = 4.00 Hz, 2H), 5.86 (t, *J* = 4.00 Hz, 1H), 4.94 (s, 2H); <sup>13</sup>C NMR (100 MHz, CD<sub>3</sub>OD):  $\delta$  ppm 161.01, 157.46, 136.74, 128.70, 128.13, 127.56, 95.98, 95.33, 70.14; MS (MALDI TOF, CHCl<sub>3</sub>): m/z 255.0182[M + K]<sup>+</sup>.

**Compound 16.** To an ice cooled solution of **8** (1.425 g, 7.7 mmol) in 30 ml of THF (dry), the solution of **15** (830 mg, 3.25 mmol) and DIPEA(1.5 ml) in 30 ml of THF was added drop wise for 2 h. After stirring for next 2.5 h reaction mixture was filtered. Filtrate and another solution of **15** (670 mg, 2.63 mmol) in THF (60 ml) were dropwise and simultaneously added to the solution of DIPEA (0.9 ml) for 3 h. Reaction was further stirred at rt for 36 h. After completion the reaction was concentrated under reduced pressure and crude was purified by silica gel (100-200 mesh) column chromatography using EA / PE (7%) as an eluent to get white solid **16** (500 mg, 11 %). TLC (20 % EA / PE ): R<sub>f</sub> 0.68; mp: 142-143 °C; IR  $\nu$  2924 (s), 2853 (m), 1629 (s), 1576 (s), 1555 (s), 1459 (s), 1404 (s), 1299 (s), 1256 (s), 1121 (s), 1021 (s); <sup>1</sup>H NMR (400 MHz, CD<sub>3</sub>):  $\delta$  ppm 7.41-7.34 (m, 10 H), 6.79-6.78 (d, *J* = 4.00 Hz, 2H), 6.68 (t, *J* = 4.00 Hz, 1H), 5.05 (s, 4H); <sup>13</sup>C NMR (100 MHz, CD<sub>3</sub>OD):  $\delta$  ppm 173.36, 170.77, 160.69, 152.02, 135.52, 128.88, 127.70, 107.40, 107.00, 70.96, 29.78; MS (MALDI TOF, CHCl<sub>3</sub>): m/z 685.0032[M + K]<sup>+</sup>

## 4.4 spectral Data:

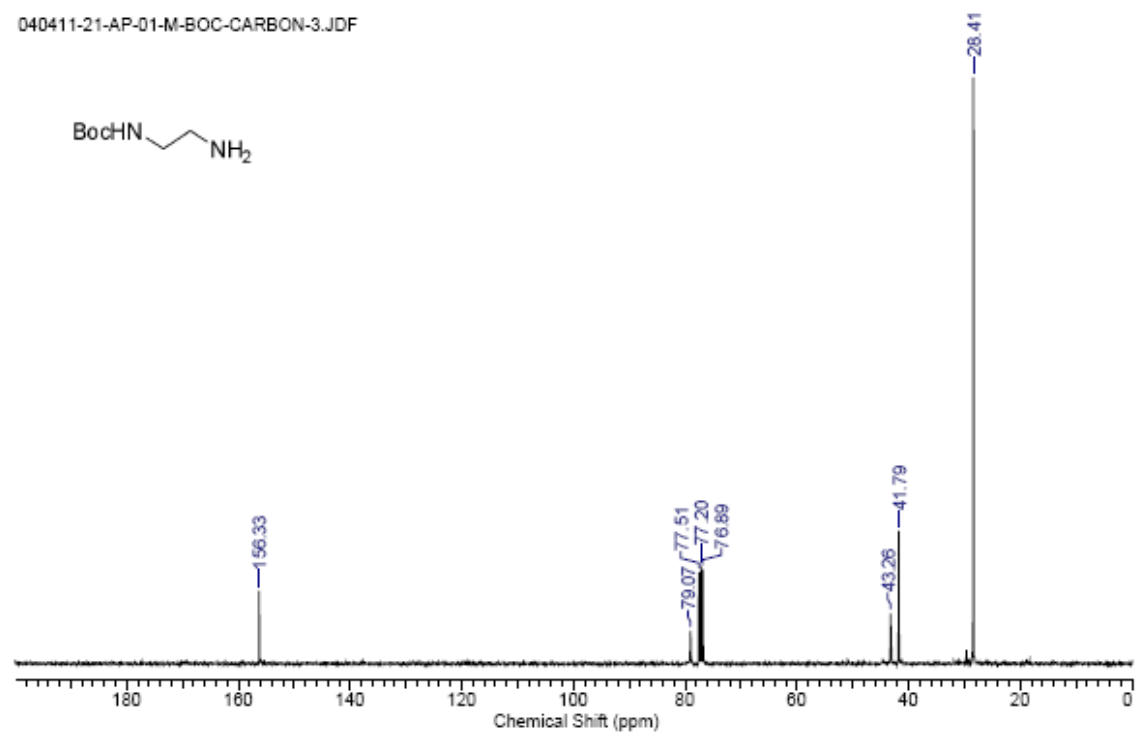
### $^1\text{H}$ NMR of compound **2**

310411-11-AP-01-M-BOC\_PROTON-3.JDF



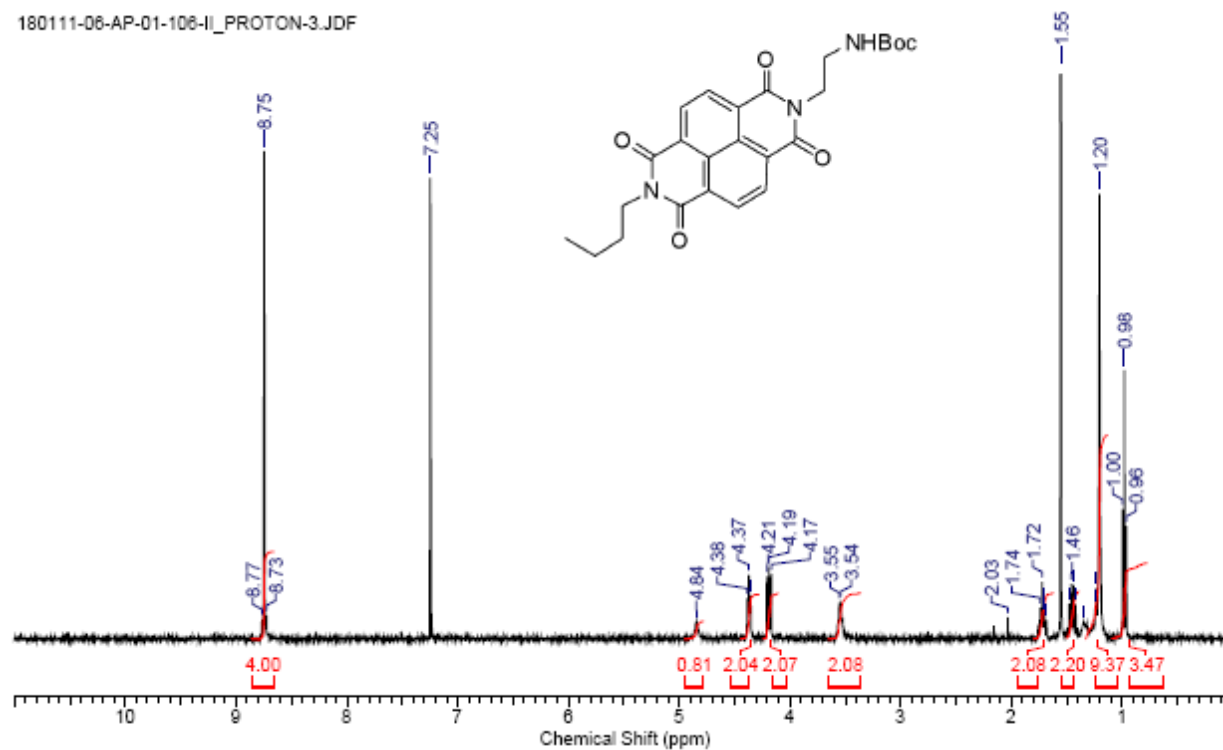
### $^{13}\text{C}$ NMR of compound **2**

040411-21-AP-01-M-BOC-CARBON-3.JDF



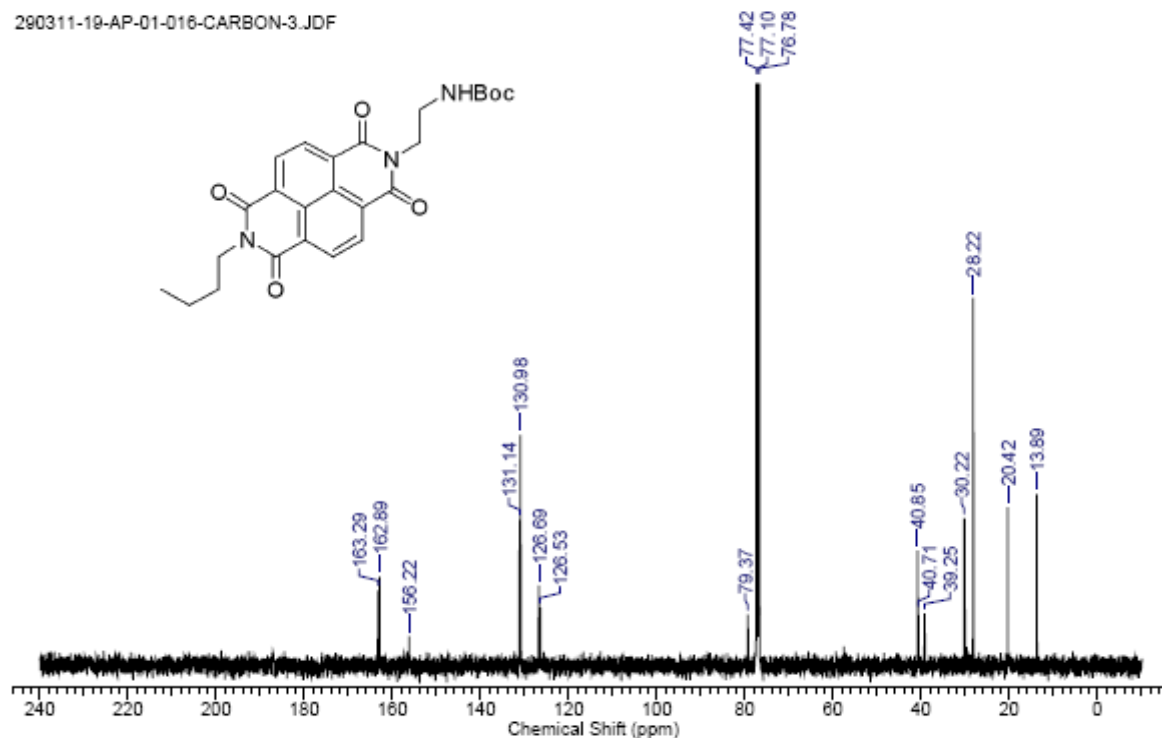
# <sup>1</sup>H NMR of compound 5

180111-06-AP-01-106-II\_PROTON-3.JDF

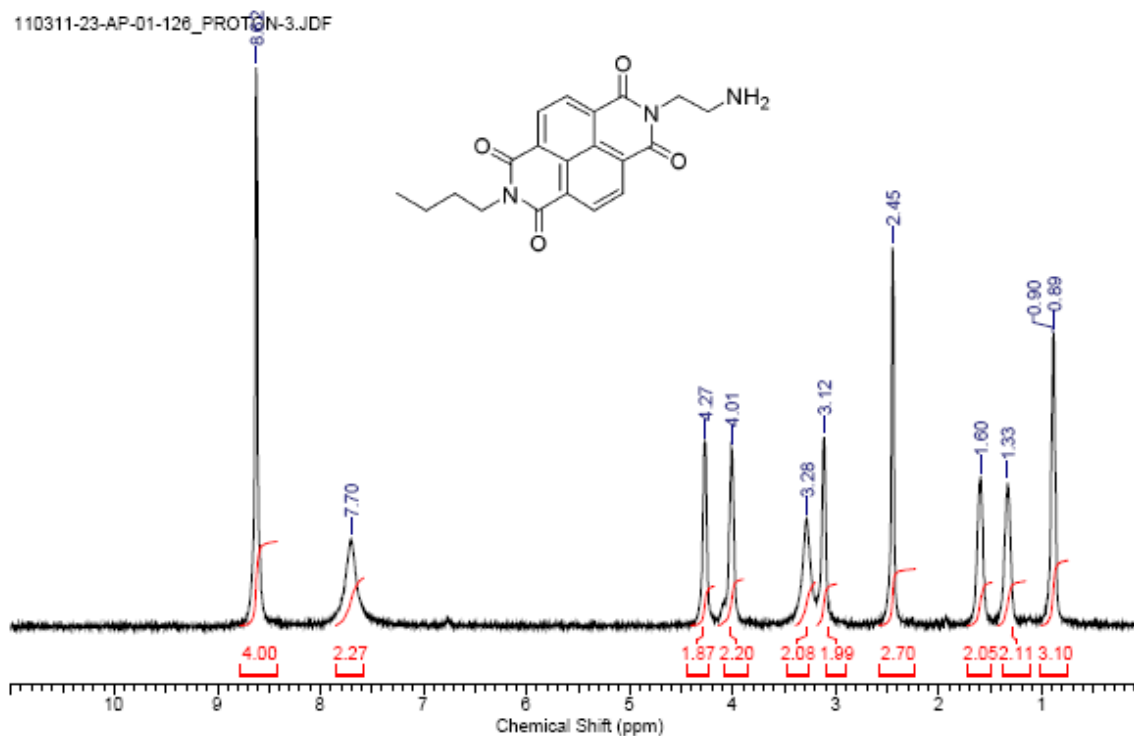


# <sup>13</sup>C NMR of compound 5

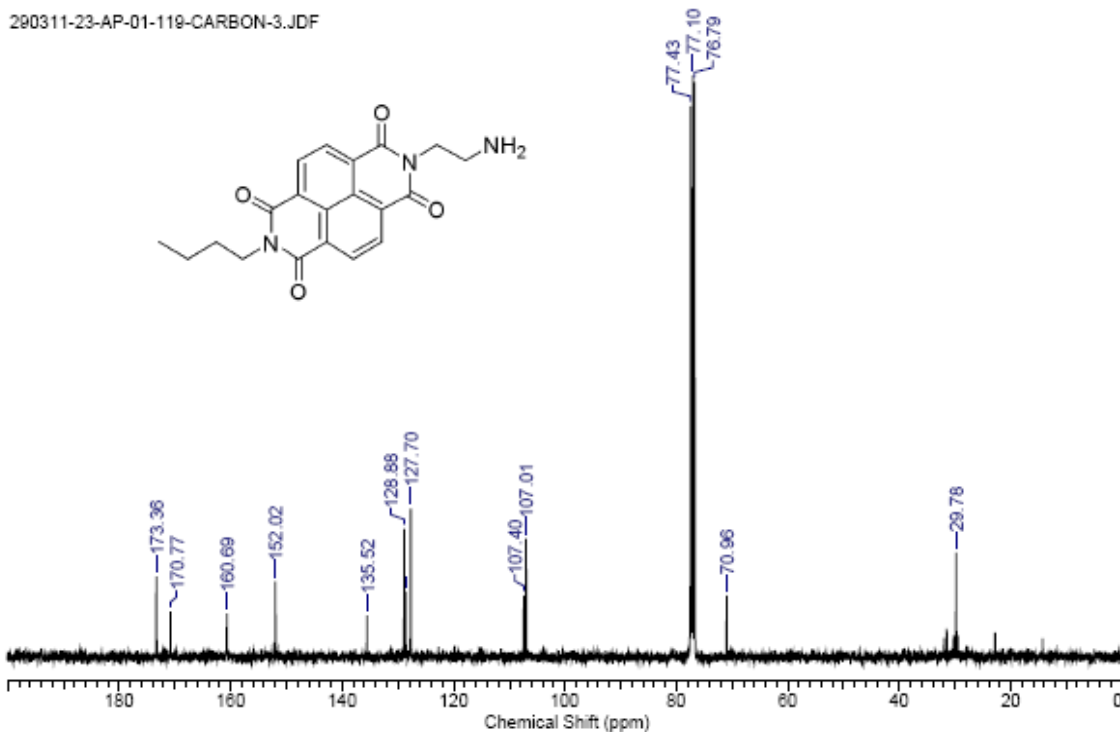
290311-19-AP-01-016-CARBON-3.JDF



# <sup>1</sup>H NMR of compound 6

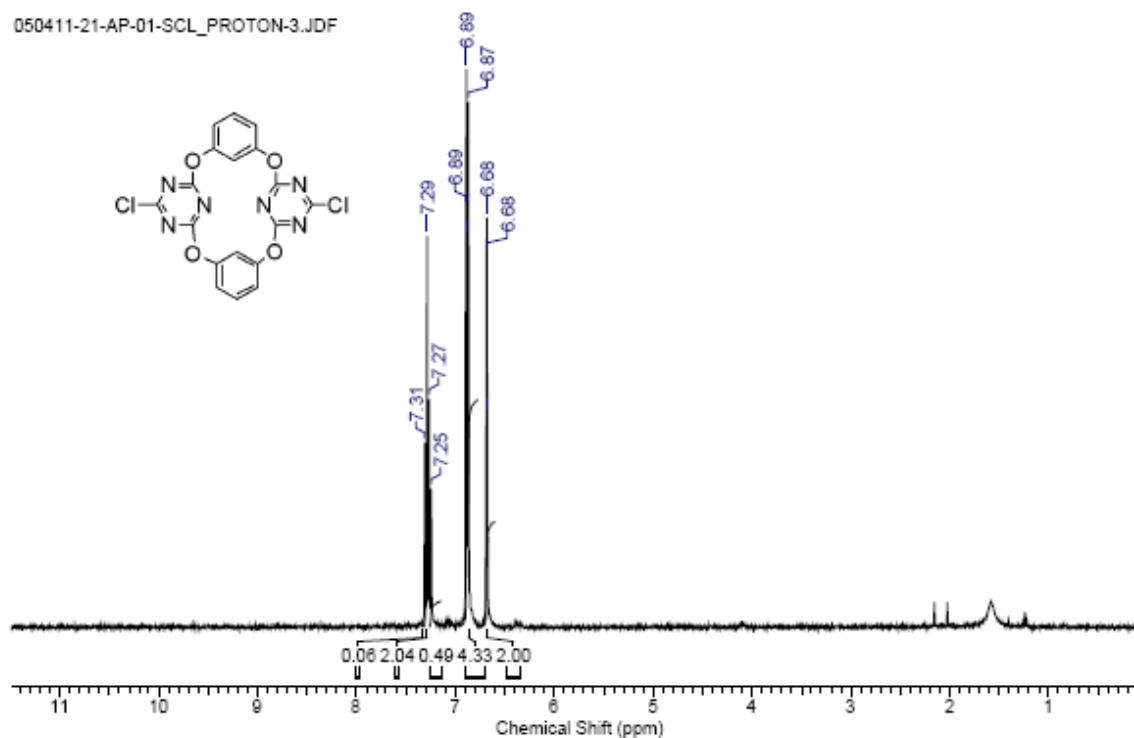


# <sup>13</sup>C NMR of compound 6



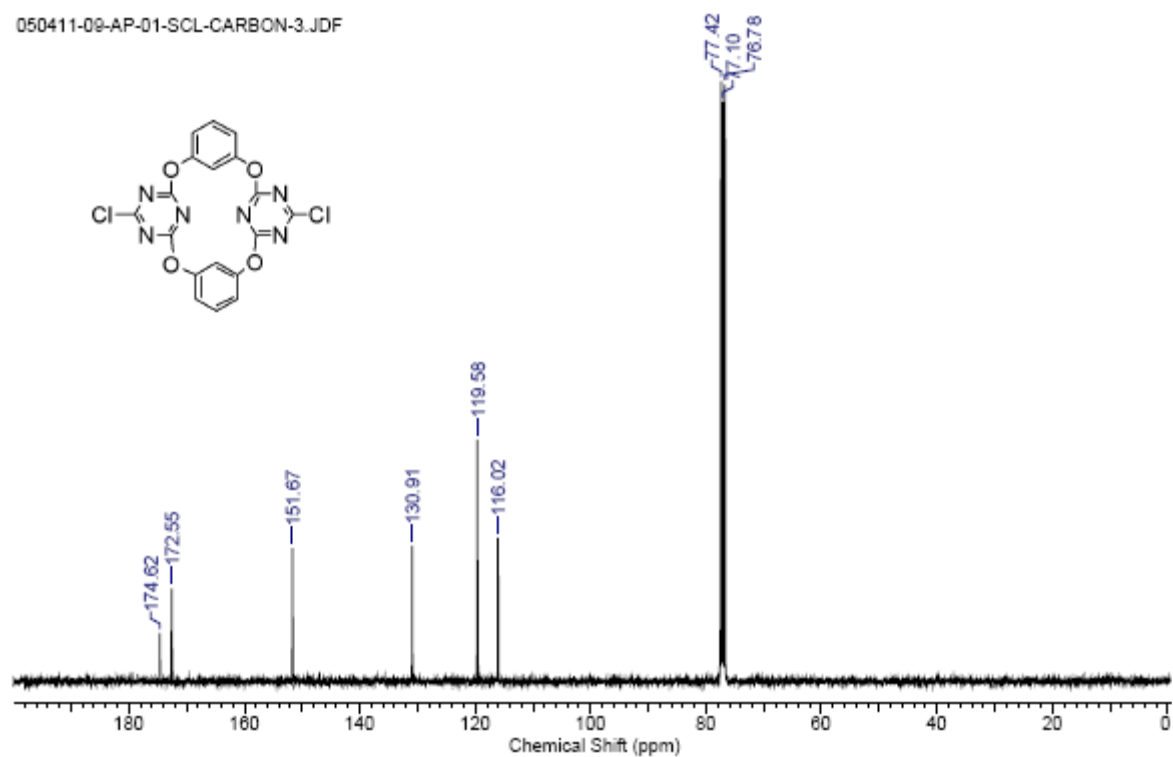
# <sup>1</sup>H NMR of compound **9**

050411-21-AP-01-SCL\_PROTON-3.JDF



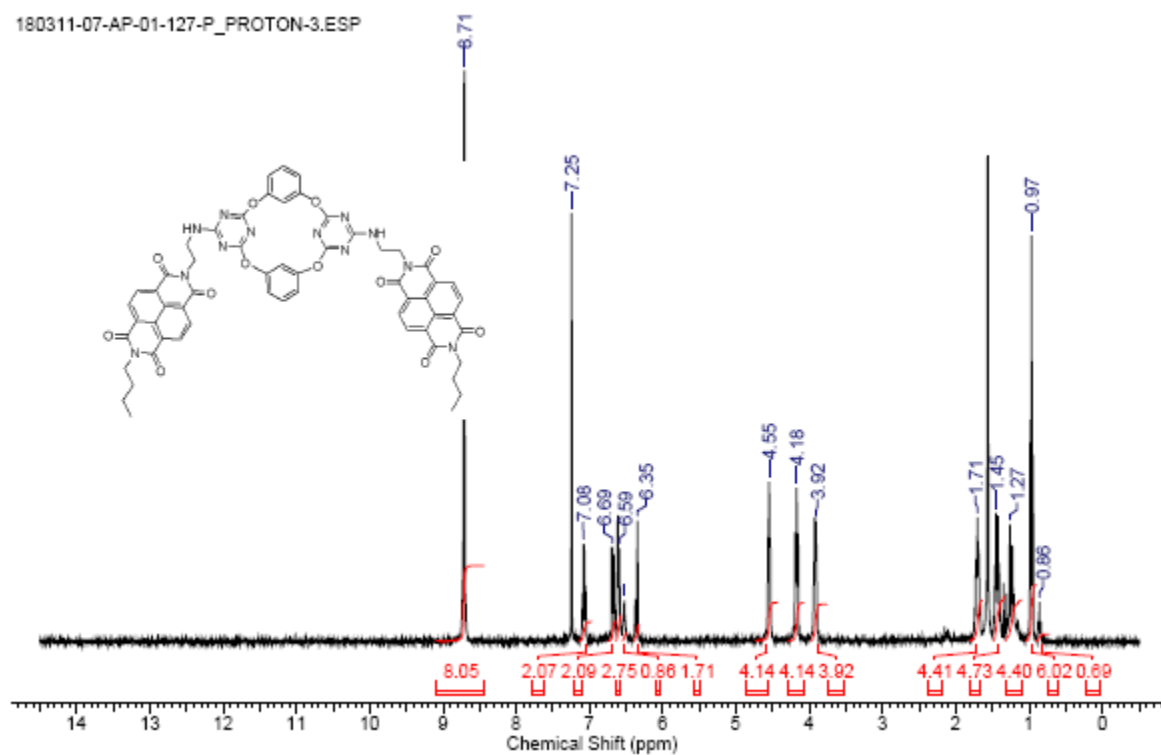
# <sup>13</sup>C NMR of compound **9**

050411-09-AP-01-SCL-CARBON-3.JDF

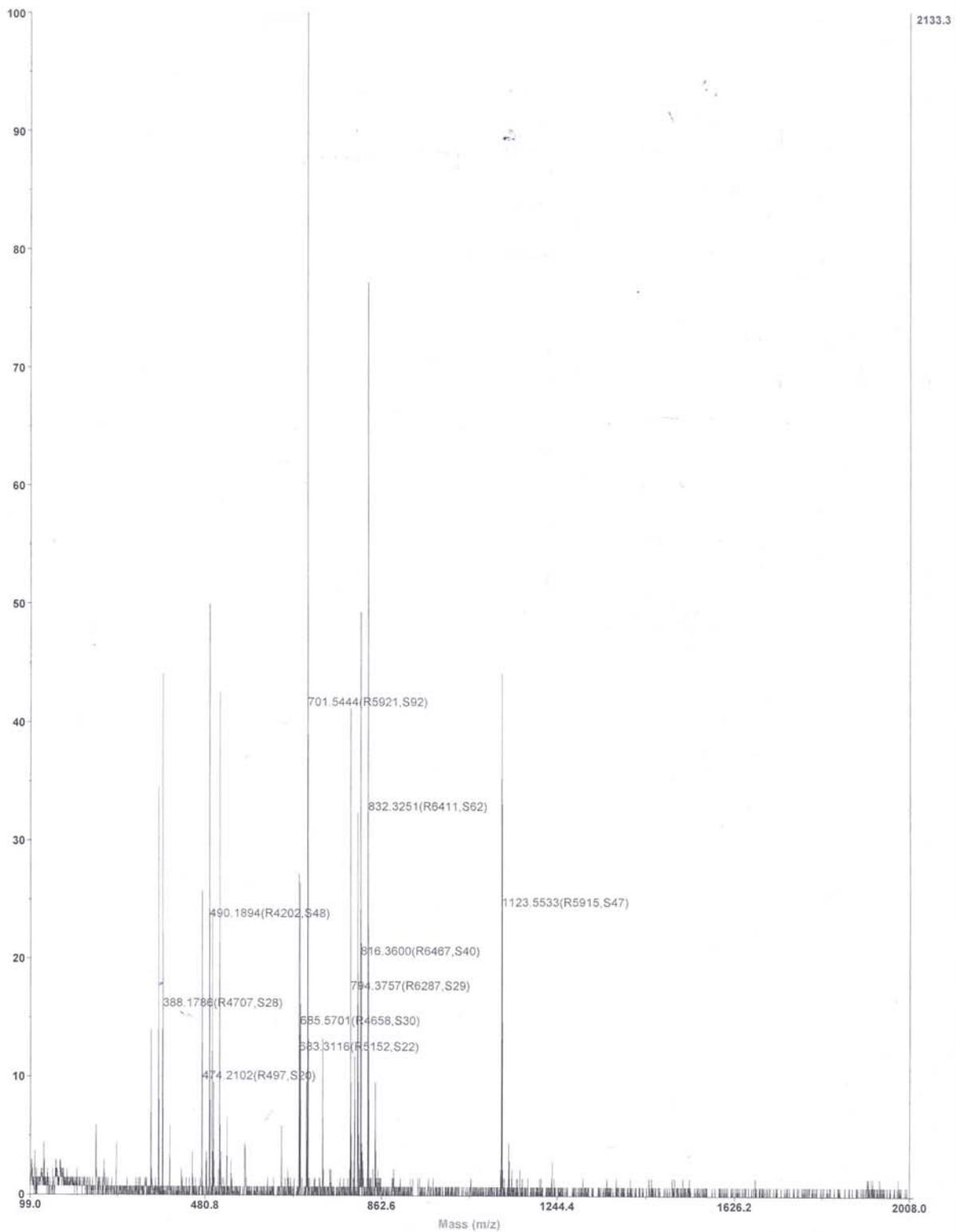


# <sup>1</sup>H NMR of compound **10**

180311-07-AP-01-127-P\_PROTON-3.ESP

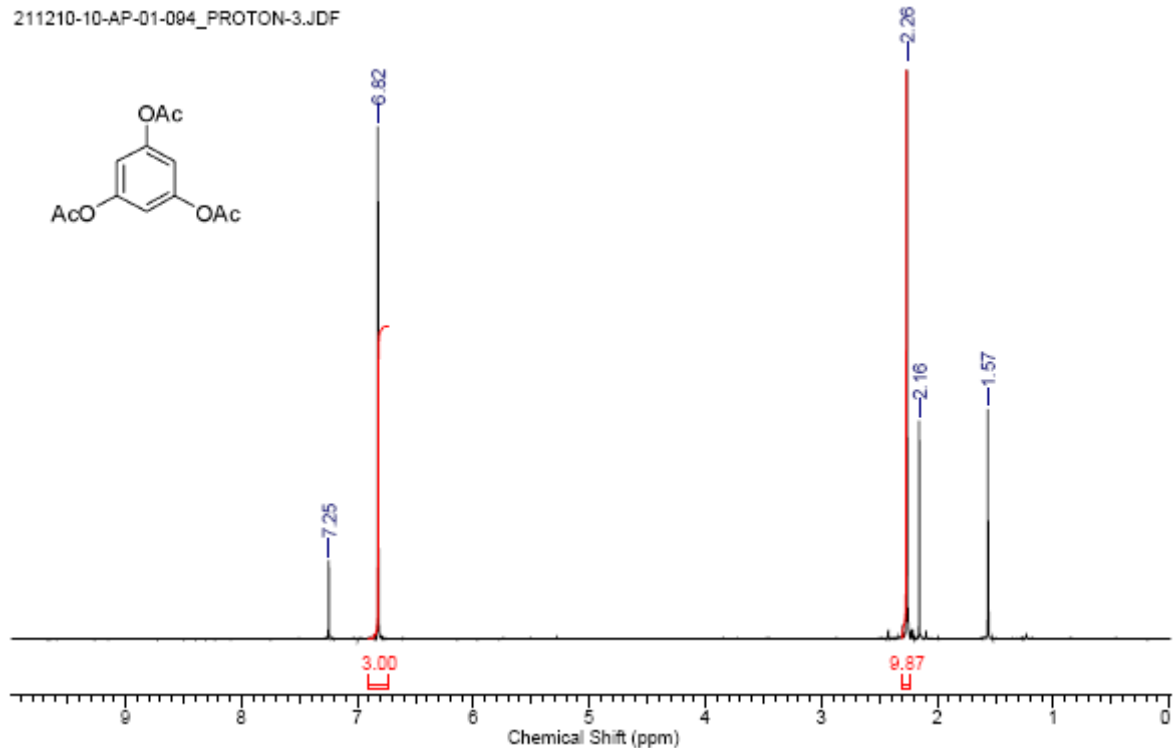


# MALDI Spectra of compound **10**. (Mol. Wt. 1101)



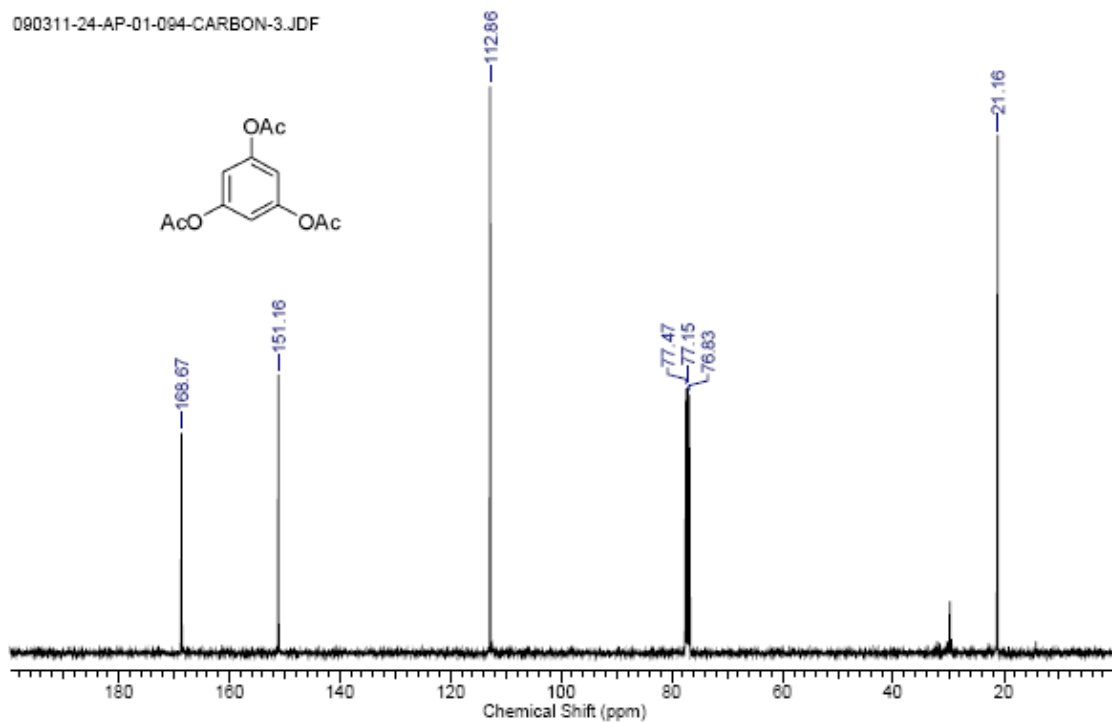
# <sup>1</sup>H NMR of compound **12**

211210-10-AP-01-094\_PROTON-3.JDF



# <sup>13</sup>C NMR of compound **12**

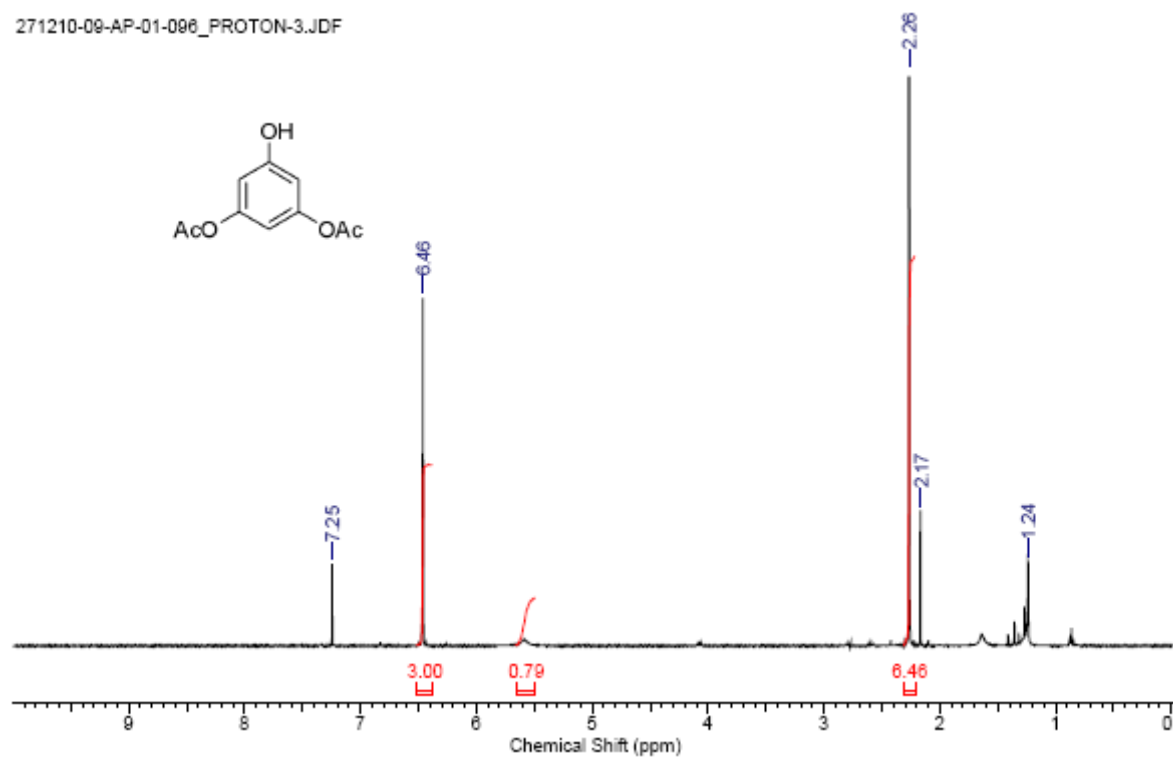
090311-24-AP-01-094-CARBON-3.JDF





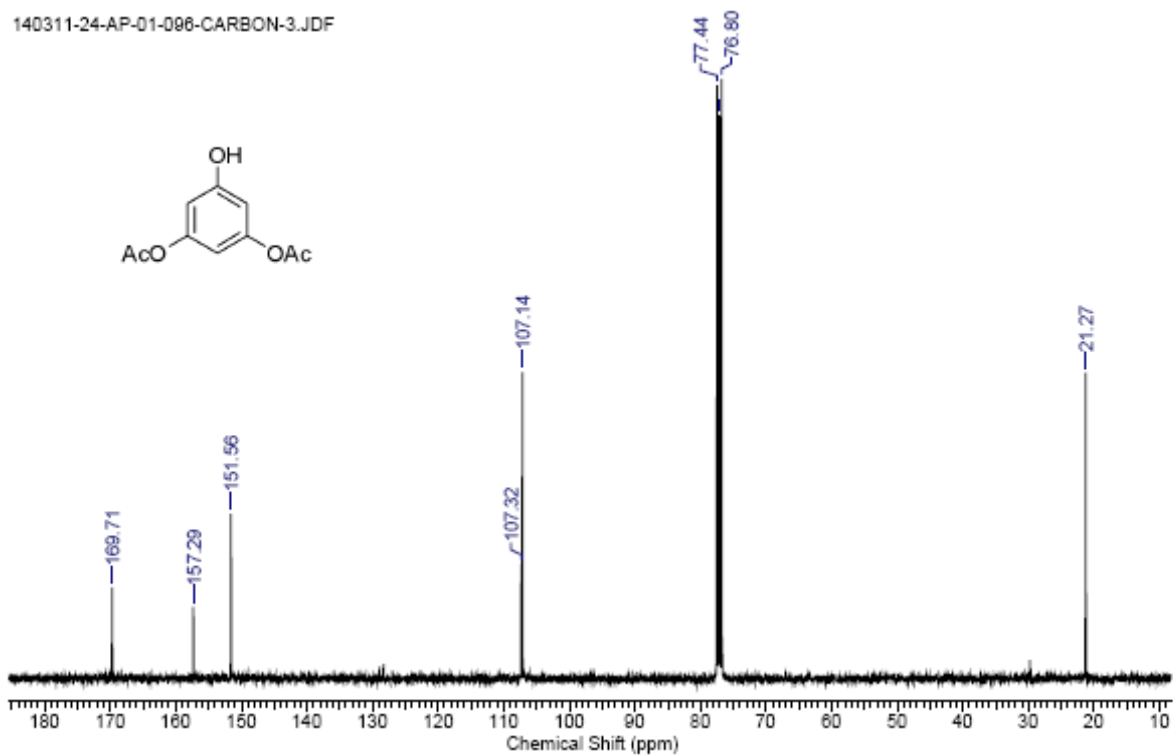
# <sup>1</sup>H NMR of compound **13**

271210-09-AP-01-096\_PROTON-3.JDF



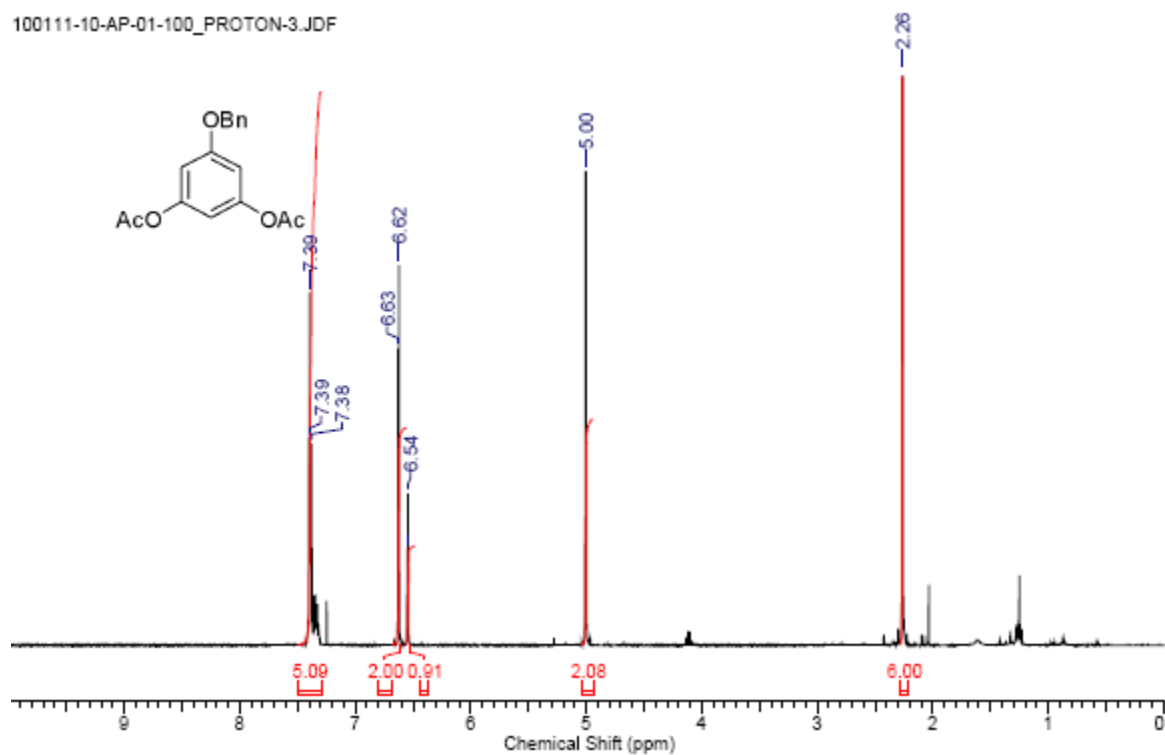
# <sup>13</sup>C NMR of compound **13**

140311-24-AP-01-096-CARBON-3.JDF



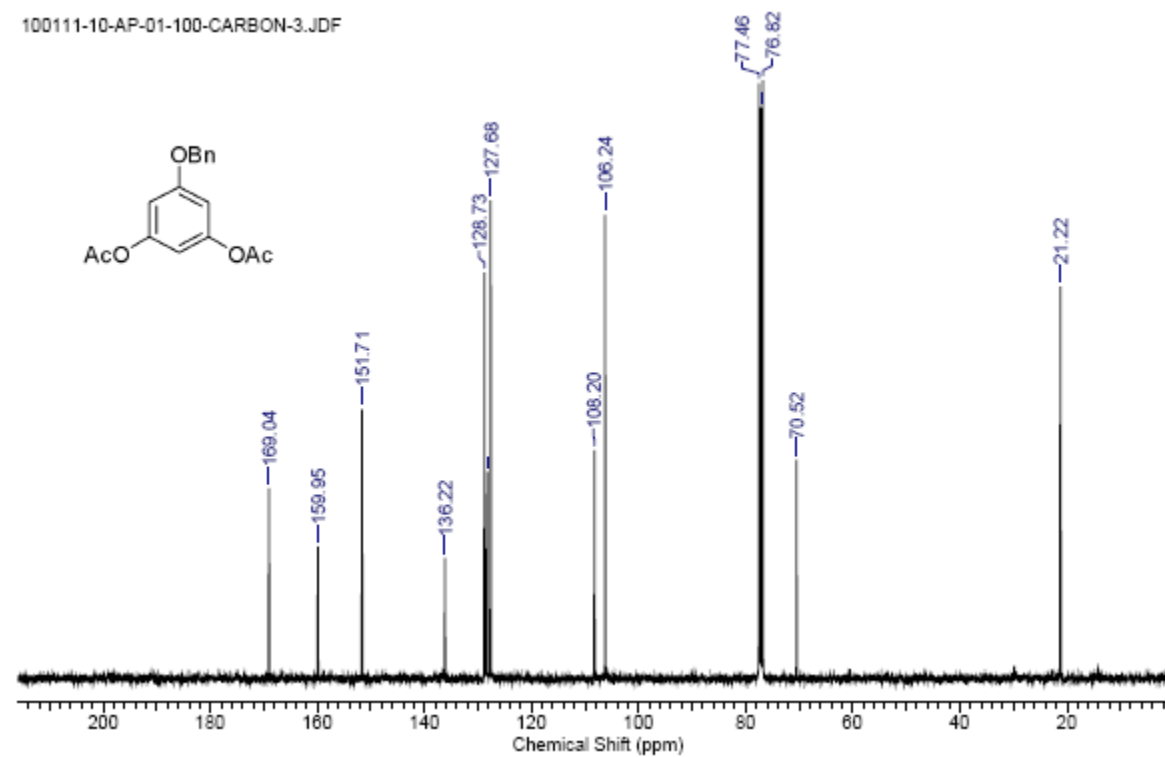
# <sup>1</sup>H NMR of compound **14**

100111-10-AP-01-100\_PROTON-3.JDF



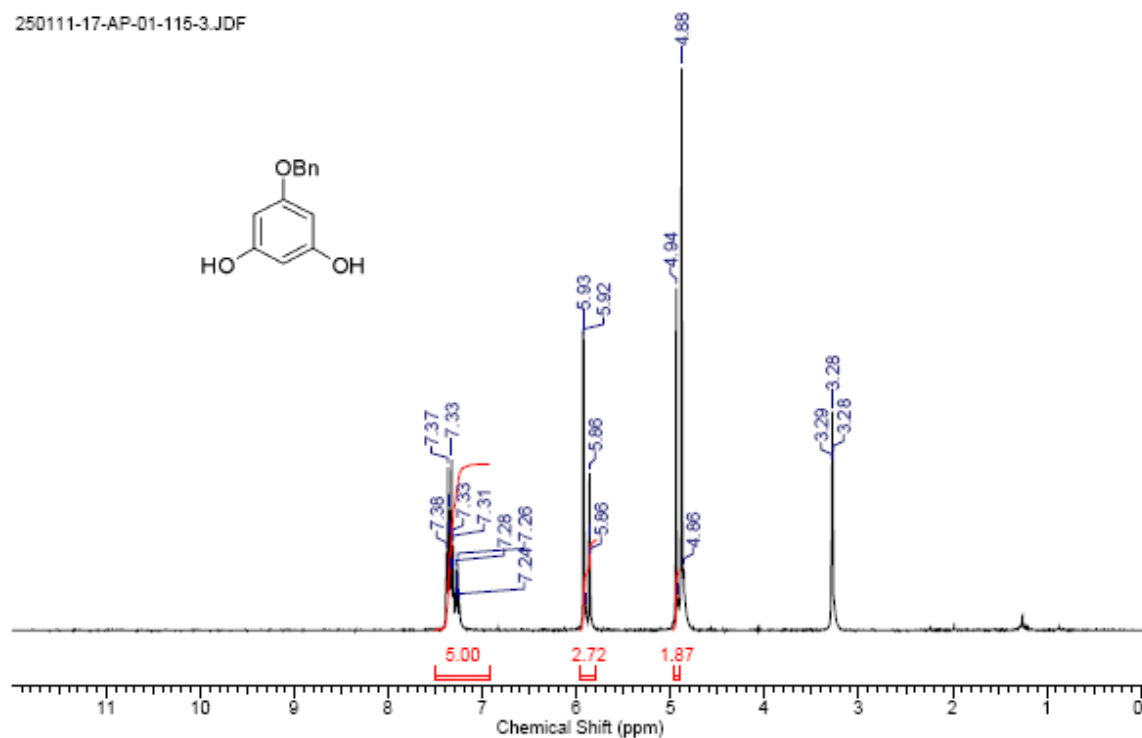
# <sup>13</sup>C NMR of compound **14**

100111-10-AP-01-100-CARBON-3.JDF



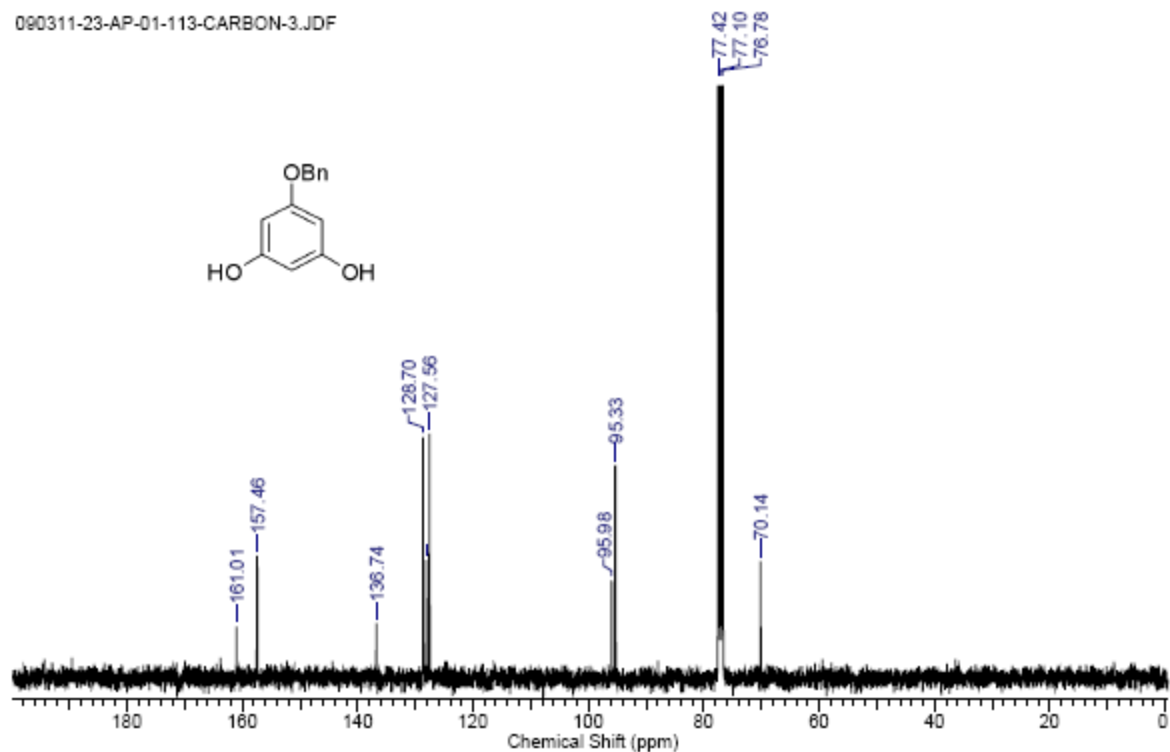
# <sup>1</sup>H NMR of compound **15**

250111-17-AP-01-115-3.JDF

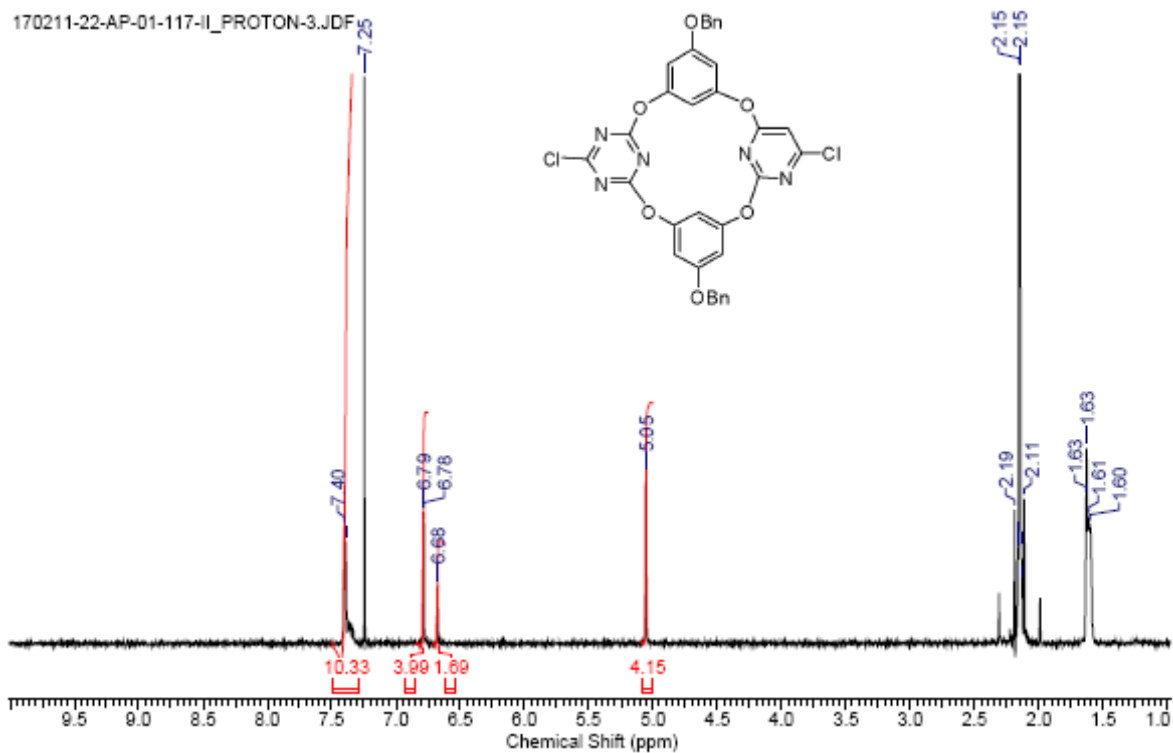


# <sup>13</sup>C NMR of compound **15**

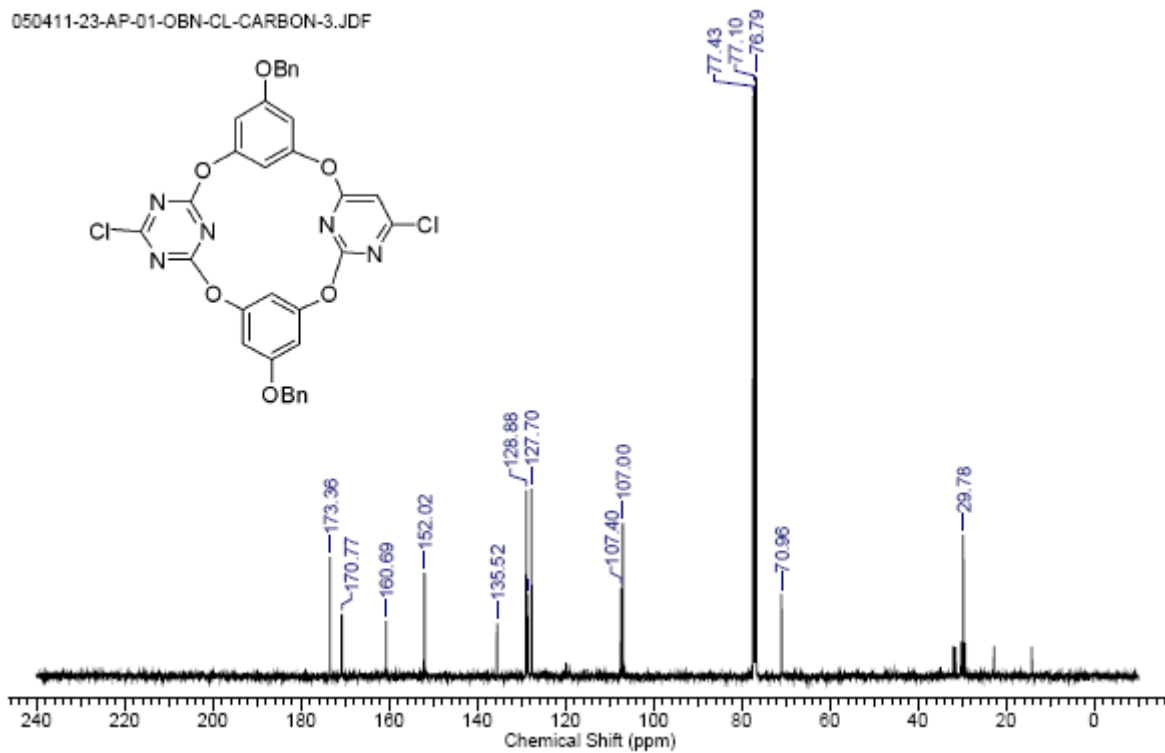
090311-23-AP-01-113-CARBON-3.JDF



# <sup>1</sup>H NMR of compound **16**



# <sup>13</sup>C NMR of compound **16**



## Chapter 5

### References:

- (1) Lehn, J.-M. *Chemical Society reviews* **2007**, *36*, 151.
- (2) Zhu, W.; Tan, X.; Shen, J.; Luo, X.; Cheng, F.; Mok, P. C.; Ji, R.; Chen, K.; Jiang, H. *Journal of Physical Chemistry A* **2003**, *107*, 2296.
- (3) Garau, C.; Frontera, A.; Quinonero, D.; Ballester, P.; Costa, A.; Deya, P. M. *Chemical Physics Letters* **2004**, *399*, 220.
- (4) Petitjean, A.; Khoury, R. G.; Kyritsakas, N.; Lehn, J.-M. *Journal of the American Chemical Society* **2004**, *126*, 6637.
- (5) Zhu, W.-L.; Tan, X.-J.; Puah, C. M.; Gu, J.-D.; Jiang, H.-L.; Chen, K.-X.; Felder, C. E.; Silman, I.; Sussman, J. L. *Journal of Physical Chemistry A* **2000**, *104*, 9573.
- (6) Felder, C.; Jiang, H.-L.; Zhu, W.-L.; Chen, K.-X.; Silman, I.; Botti, S. A.; Sussman, J. L. *Journal of Physical Chemistry A* **2001**, *105*, 1326.
- (7) Mo, Y.; Subramanian, G.; Gao, J.; Ferguson, D. M. *Journal of the American Chemical Society* **2002**, *124*, 4832.
- (8) Nicholas, J. B.; Hay, B. P.; Dixon, D. A. *Journal of Physical Chemistry A* **1999**, *103*, 1394.
- (9) Tedesco, M. M.; Ghebremariam, B.; Sakai, N.; Matile, S. *Angewandte Chemie, International Edition* **1999**, *38*, 540.
- (10) Gamez, P.; Mooibroek, T. J.; Teat, S. J.; Reedijk, J. *Accounts of Chemical Research* **2007**, *40*, 435.
- (11) Demeshko, S.; Dechert, S.; Meyer, F. *Journal of the American Chemical Society* **2004**, *126*, 4508.
- (12) Maeda, H.; Osuka, A.; Furuta, H. *Journal of Inclusion Phenomena and Macrocyclic Chemistry* **2004**, *49*, 33.
- (13) Schottel, B. L.; Chifotides, H. T.; Dunbar, K. R. *Chem. Soc. Rev.* **2008**, *37*, 68.
- (14) Alkorta, I.; Rozas, I.; Elguero, J. *Journal of the American Chemical Society* **2002**, *124*, 8593.
- (15) de Hoog, P.; Gamez, P.; Mutikainen, I.; Turpeinen, U.; Reedijk, J. *Angewandte Chemie, International Edition* **2004**, *43*, 5815.
- (16) Gorteau, V.; Bollot, G.; Mareda, J.; Perez-Velasco, A.; Matile, S. *Journal of the American Chemical Society* **2006**, *128*, 14788.
- (17) Rosokha, Y. S.; Lindeman, S. V.; Rosokha, S. V.; Kochi, J. K. *Angewandte Chemie, International Edition* **2004**, *43*, 4650.
- (18) Seto, C. T.; Whitesides, G. M. *Journal of the American Chemical Society* **1993**, *115*, 905.
- (19) Yang, H.-B.; Wang, D.-X.; Wang, Q.-Q.; Wang, M.-X. *Journal of Organic Chemistry* **2007**, *72*, 3757.